EIDESSTATTLICHE ERKLÄRUNG

AFFIDAVIT

Ich erkläre an Eides statt, dass ich die vorliegende Arbeit selbstständig verfasst, andere als die angegebenen Quellen/Hilfsmittel nicht benutzt, und die den benutzten Quellen wörtlich und inhaltlich entnommenen Stellen als solche kenntlich gemacht habe. Das in TUGRAZonline hochgeladene Textdokument ist mit der vorliegenden Masterarbeit identisch.

I declare that I have authored this thesis independently, that I have not used other than the declared sources/resources, and that I have explicitly indicated all material which has been quoted either literally or by content from the sources used. The text document uploaded to TUGRAZonline is identical to the present master‘s thesis.

Datum / Date

Unterschrift / Signature

Wer will, dass die Welt so bleibt wie sie ist, der will nicht, dass sie bleibt.

Erich Fried (1921 - 1988)

Acknowledgement

First of all, I would like to express my gratitude to my great supervisor Prof. Eduard Paschke, who gave me the opportunity to work on this project in the first place. I want to thank him for his continuous support throughout the course of the master's thesis, for his patience, cordiality as well as for the contribution of his immense knowledge.
Furthermore, I want thank Dr. Günter Fauler for his great support regarding the analytical part of this thesis. Without his precise advices and prodigious knowledge in the field of analytical chemistry – which he was eager to share – the method development would not have worked out the way it did. I am also grateful to Bettina Pabst for her competent help regarding the cell cultures.
A special thanks goes to my colleagues Thomas Kaiser and Benno Amplatz. As we all worked on the same instruments, albeit on different premises, the exchange of experiences and the mutual assistance were priceless. I also want to thank them for all the stimulating discussions we had, both in the lab and after work.
I also want to thank all the other people in the Paschke-, Fauler- and Leis-Lab whom I didn't mention before. It was a pleasure working with you.

Last but not least I want to thank my parents and family for their undivided support and encouragement throughout my studies. I will be grateful forever for your love.

Zusammenfassung

Die lysosomale β-Galactosidase (ß-gal) katalysiert die Hydrolyse terminaler ß-galactosidischer Bindungen in Sphingolipiden (Ganglioside G_{M1} und G_{A1}), N- und O-glykosidischen Oligosacchariden und dem Glykosaminoglykan Keratansulfat. Mutationen im Strukturgen dieses Enzyms haben sehr unterschiedliche Auswirkungen und können zwei lysosomale Speichererkrankungen, G_{M1}-Gangliosidose (GM1) und Morbus Morquio Typ B (Morquio B disease, MBD) hervorrufen. GM1 manifestiert sich durch Störungen der Skelettentwicklung und durch Defekte im Zentralnervensystem, Patienten mit MBD entwickeln eine charakteristische Skelettdysplasie („Dysostosis multiplex“), sind aber völlig frei von neurologischen Symptomen.

Verschiedene der etwa 50 lysosomalen Speichererkrankungen können bisher durch Ersatz des defekten Enzyms, zum Beispiel durch Transplantation hämatopoetischer Stammzellen oder Infusion rekombinanter Enzympräparate („Enzymersatztherapie“ (ERT)) therapiert werden. Für Defekte des GLB1-Gens ist dies wenig aussichtsreich, da Proteine wegen der Blut-Hirn-Schranke das Zentralnervensystem nicht erreichen können. Als Alternative wurde der Einsatz kleiner Moleküle vorgeschlagen. Diese „pharmakologischen Chaperones“ sollen an das aktive Zentrum der mutierten Enzymvorstufen im ER binden, ihre normale Struktur und ihren Transport ins lysosomale Kompartiment ermöglichen, sodass die enzymatische Aktivität zumindest partiell wiederhergestellt werden kann.

Zum Nachweis dieses Effektes werden Substanzen mit möglicher Chaperonwirkung dem Kulturmedium von kultivierten Zellen von GM1- oder MBD-Patienten zugesetzt und die Aktivität des defekten Enzyms geprüft. Eine positive Chaperonwirkung liegt vor, wenn ein Anstieg der Aktivität der ß-gal auf den 3-fachen Ausgangswert oder zumindest 10% der Aktivität normaler Kontrollzellen zu beobachten ist.

Wenig ist dabei allerdings bisher über das intrazelluläre Schicksal pharmakologischer Chaperons bekannt, d.h. es gibt bisher wenig Daten über die tatsächlich aufgenommenen, intrazellulär wirksamen Konzentrationen oder über ihre subzelluläre Verteilung.

In der Masterarbeit wurde daher primär eine Methode entwickelt mit der das

pharmakologische Chaperon DLHex-DGJ in Homogenaten und subzellulären Fraktionen kultivierter Hautfibroblasten mittels Tandem –Massenspektrometrie quantitativ bestimmt werden kann (MDL 1,15 ng/ml; MQL 3,59 ng/ml).

Zur Bestimmung von Aufnahmekinetik und intrazellulärem Umsatz wurde die Konzentrations- und Zeitabhängigkeit der Aufnahme von DLHex-DGJ in kultivierte Hautfibroblasten mit einer bekannten, Chaperon-sensitiven Mutation – p.R201C – untersucht und mit Fibroblasten des Wildtyps verglichen. Es konnte gezeigt werden, dass die Aufnahme von DLHex-DGJ bei einer Konzentration von 20 – 500 µM im Nährmedium einer linearen Kinetik folgt. Wenige Stunden nach Zugabe wird eine stabile intrazelluläre Konzentration erreicht und nach Entfernen des Chaperones aus dem Kulturmedium folgt die Abnahme der gleichen, raschen Kinetik, ohne dass es Anzeichen von Speicherung oder intrazellulärem Einschluss gibt. Weiters konnte gezeigt werden, dass die Aktivitätssteigerung der β-Galactosidase sofort nach der ersten Zugabe des Chaperones eintritt und nach Entfernung von DLHex-DGJ aus dem Nährmedium innerhalb von 12h auf 5,9% der Normalaktivität linear abnimmt.

Eine Analyse der Enzymreifung mittels Western Blots in dieser ersten Phase der Chaperone-Zugabe zeigt, dass es zuerst zu einer Zunahme von Abbauprodukten des Precursor-Enzymes kommt, bevor gesteigerte Mengen an reifem Enzym detektierbar sind.

Schließlich konnten Voruntersuchungen zur subzellulären Lokalisierung von DLHex-DGJ mittels „Digitonin –Titration“ durchgeführt werden. Es zeigte sich eine weitgehende Parallelität in der Freisetzung des lysosomalen Markers ß-Hexosaminidase und DLHex-DGJ nach Digitoninbehandlung. Dies deutet darauf hin, dass DLHex-DGJ in der Zelle vornehmlich im lysosomalen Kompartiment akkumuliert.

Zusammenfassend konnte diese Arbeit neue Einblicke in den zellulären Mechanismus von pharmakologischer Chaperonetherapie sowie deren Effekt auf die Zielenzyme bereitstellen, was zur Entwicklung neuer, besser wirksamer Chaperone-Substanzen beitragen kann.

Abstract

Human lysosomal β-galactosidase, part of a multienzyme complex, degrades terminal β-linked galactose residues from macromolecules such as G_{M1}-gangliosides, N- and O-linked oligosaccharides as well as keratane sulfates in the lysosomal compartment. Mutations in its structural gene, *GLB1*, can cause either G_{M1}-gangliosidosis (GM1) or Morquio B disease (MBD). GM1 becomes manifest in a disruption of the skeletal development as well as in defects of the central nervous system, while patients suffering from Morquio B disease develop characteristic skeletal dysplasia ("dysostosis multiplex") but are entirely free of neurological symptoms.

Some of the approximately 50 lysosomal storage disorders can be treated via replacement of the affected enzyme, e.g. by transplantation of hematopoietic stem cells or infusion of recombinant enzymes (enzyme replacement therapy (ERT)). For defects in *GLB1* this approach is not promising, as proteins cannot reach the central nervous system due to the blood-brain barrier. Alternatively the use of small molecules has been proposed. Those pharmacological chaperones should bind to the active center of the mutant enzyme-precursors in the ER and hence enable their normal folding as well as the transport to the lysosomal compartment. This should at least partially restore their enzymatic activity.

To detect the effects of potential chaperone-substances, they are administered to the culture medium of cultivated cells from GM1- and MBD-patients and the enzymatic activity is tested. A positive chaperone-activity is achieved if the restoration of ß-gal-activity triples the initial value or reaches at least 10% of the activity of control cells.

However, up to now little is known on the intracellular fate of those pharmacological chaperones. There is only little data available on the amount of substance which is effectively taken up by cells and on its subcellular localization.

Therefore, in the course of this master's thesis, a method was developed to quantitatively detect the pharmacological chaperone DLHex-DGJ in homogenates and subcellular fractions of cultured skin fibroblasts by tandem mass spectrometry (MDL 1,15 ng/ml; MQL 3,59 ng/ml).

In order to test for uptake kinetics and chaperone turnover, dependence on

concentration and time of the uptake of DLHex-DGJ in cultured skin fibroblasts was examined in the known-to-be chaperone sensitive p.R201C mutant and compared to wildtype fibroblasts. It could be shown that the uptake of DLHex-DGJ in cultured fibroblasts follows a linear kinetic at concentrations between 20 and 500 µM in the culture medium. A stable intracellular concentration is reached just after a few hours and after removal of the chaperone from the culture medium, the release of DLHex-DGJ follows the same, rapid kinetics, showing no signs of entrapment or storage. Restoration of β-galactosidase activity was shown to take place almost immediately after the first chaperone administration and declines linearly to 5,9% of its normal activity within 12 hours after the chaperone is removed from the culture medium.

Examination of the enzyme-maturation with western blots showed that in this first phase of chaperone-administration, degradation products of the precursor enzyme are generated before an increased amount of mature enzyme can be detected.

Finally, preliminary investigations on the subcellular localization of DLHex-DGJ were done via „digitonin-titration“. The release of DLHex-DGJ showed extensive conformity with the lysosomal marker ß-hexosaminidase after digitonin treatment. This points to the fact that DLHex-DGJ primarily accumulates in the lysosomal compartment of cells.

Taken together, this current work reveals insights into the cellular mechanisms of pharmacological chaperoning and its effects on target proteins and should promote the development of novel, more effective chaperone substances.

Table of Contents

1 Abbrevations

DLHex-DGJ	Methyl-{[N2-(dansyl)-N6-(1,5-dideoxy-D-galactitol-1,5-diyl)-L-lysyl]amino} hexanoate
EET	Enzyme enhancement therapy
ERT	Enzyme replacement therapy
ESI	Electrostpray ionization
GAG	Glycosaminoglycan
HPLC	High performance liquid chromatography
LDH	Lactate dehydrogenase
LOD	Limit of detection
LOQ	Limit of quantification
LSD	Lysosomal storage disorder
m/z	Mass-to-charge ratio
MDL	Method detection limit
MPS	Mucopolysaccharidoses
MQL	Method quantification limit
MS	Mass spectrometry
MS/MS	Tandem mass spectrometry
MS^2	Tandem mass spectrometry

PC	Pharmacological chaperone
SIM	Single ion monitoring
SPE	Solid phase extraction
SRT	Substrate restriction/reduction therapy
TIC	Total ion current
T_R	Retention time
WB	Western blot
XIC	Extracted ion current
β-GAL	β-galactosidase
β-HEX	β-hexosaminidase

2 Introduction

2.1 The lysosome and lysosomal storage disorders

Lysosomes and the related system of endosomal membranes play a major role in the metabolic network of eukaryotic cells. The centerpiece of this remarkable intracellular network is represented by the lysosome itself, an acidic, membrane-bound organelle with the main purpose to degrade and reprocess a vast number of intracellular products. Embedded in the complex array of cellular networks and metabolic pathways, it is more of a center rather than the endpoint of many cellular processes. This starts from secretory streams, transporting newly synthesized enzymes and proteins to lysosomes, on to endosomal and retrosomal streams, important parts of signal transduction and related processes, culminating in autophagic streams, conveying intracellular material for lysosomal degradation, and ending in salvage streams, allowing the egression of lysosomaly degraded products to other sites of the cell for further utilization.

The lysosomal lumen contains hydrolytic enzymes with optimal activity at an acidic pH, and the capability of degrading the majority of cellular macromolecules, including proteins, lipids, polysaccharides as well as DNA and RNA. Resulting degradation products are subsequently transported through the lysosomal membrane, often with the aid of specific transporter proteins, and provided to other cellular organelles for use in biosynthetic processes.
During the past decades it has become more and more apparent that the lysosomal system plays a pivotal role in cellular metabolic homeostasis, rather than functioning as a terminal degradation compartment. This has, for instance, recently been emphasized by the finding of the CLEAR (Coordinated Lysosomal Expression and Regulation), an overreaching network of gene regulation, showing the linkage of the greater lysosomal system on a transcriptional level [1].

Accordingly, any malfunction in the lysosomal network may lead to catastrophic consequences for cells, organs and individuals. Up to now, over 50 different types of lysosomal storage disorders have been characterized, with a cumulative incidence of approximately 1:7000 live births.

Historically, lysosomal storage diseases were initially defined as disorders resulting from deficiencies in particular lysosomal hydrolases and the subsequent accumulation of their specific substrates. Thereafter, this concept had to be extended to other lysosomal and non-lysosomal proteins, like non-lysosomal enzymes, soluble non-enzymatic and/or membrane-associated proteins of relevance for the proper function of the lysosomal system.

The majority of LSDs manifest in late infancy or early childhood, although age of onset and clinical course varies notably among individuals. Most commonly, they show delayed non-congenital onset and a progressive deterioration of multiple organ systems which ultimately leads to premature death.

The grouping of lysosomal disorders is challenging, as several diseases show significant overlapping in terms of affected proteins, pathological features, storage material etc. Classification depending on the primary storage material is therefore often preferred, resulting in categories like lipidoses, mucopolysaccharidoses (MPSs), glycogenoses, mucolipidoses, neuronal ceroid lipofuscinoses and others [2], [3].

To illustrate parts of the variety of LSDs, figure 1 gives a general overview on the sphingolipid degradation pathways and associated LSDs.

In the specific case addressed in this master's thesis, affection of one enzyme – the lysosomal β-galactosidase – may lead to two distinctly different disorders, that is G_{M1}-gangliosidosis and mucopolysaccharidosis type IV B, also termed Morquio B disease.

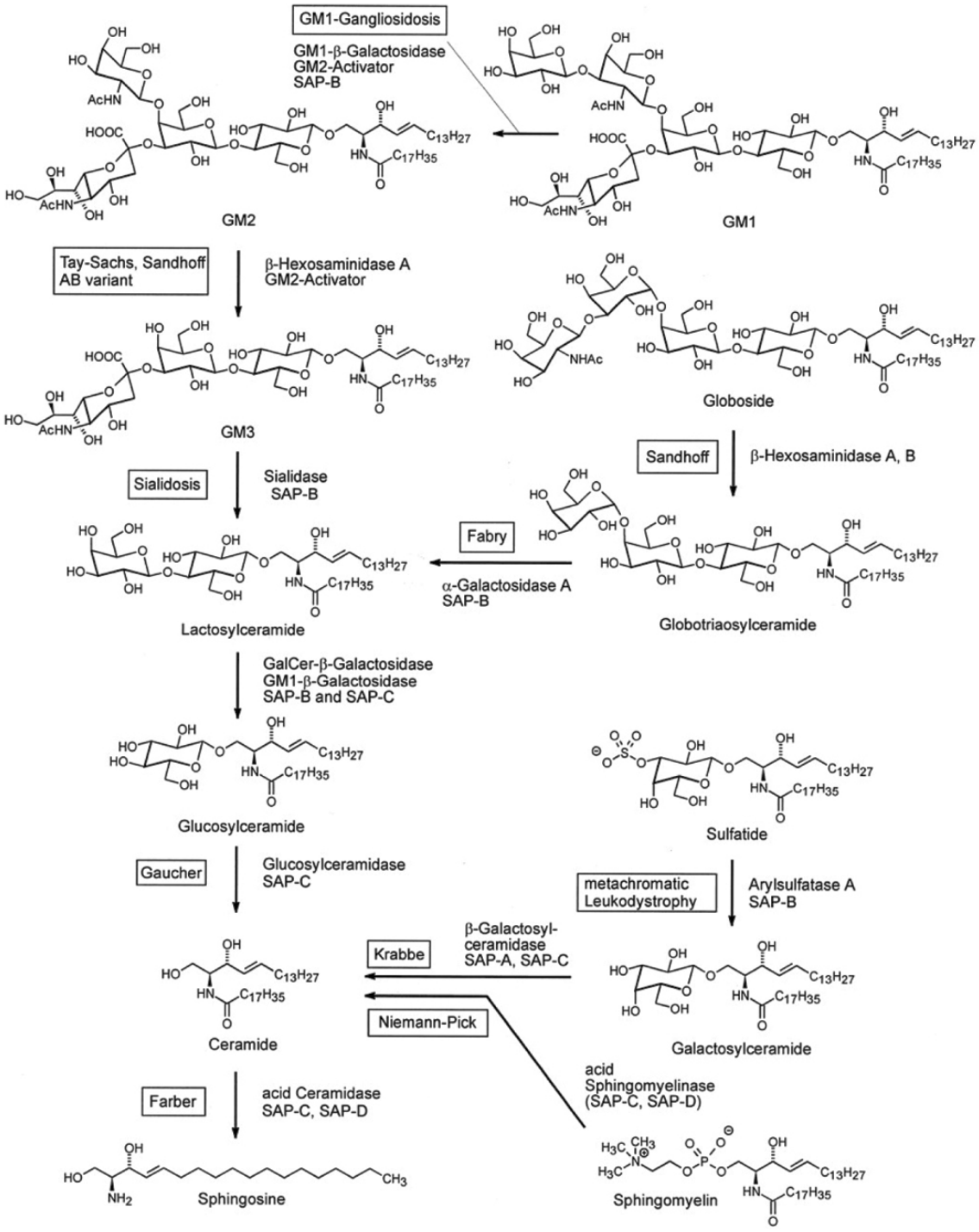

Figure 1: Overview of the degradation pathways of selected sphingolipids associated with lysosomal storage disorders

Source: http://www.lipidomicnet.org/index.php/Glycosphingolipids [59]

2.1.1 β-Galactosidase

Human lysosomal β-galactosidase, encoded by the gene *GLB1* (chromosome 3p21.33),

degrades terminal β-linked galactose residues from macromolecules such as G_{M1}-gangliosides, N- and O-linked oligosaccharides as well as keratane sulfates in the lysosomal compartment. It is known to form a complex with neuraminidase, protective protein/cathepsin A and N-acetylgalactosamine-6-sulfatase [4], [5].

The three-dimensional structure of human β-galactosidase has been determined via x-ray crystallography in 2012, which opened the gate to new insights into the functionality of the enzyme as well as the effects of different classes of mutations and the potential mechanistic principles of different forms of therapy [6].

The gene *GLB1* is located on chromosome 3 and stretches over a range of 2379 base-pairs. It is composed of 16 exons and yields three functionally relevant isoforms: Firstly lysosomal β-galactosidase, with an amino-acid count of 677 in its premature form and 649 in its processed form respectively, lacking a signal peptide part from amino acid 1 to 23 as well as a pro-peptide part from amino acid 24 to 28. Secondly, a shortened version lacking amino acids 1 to 30 which still needs to be confirmed experimentally and finally beta-galactosidase-like protein, also termed elastin-binding protein, comprising a total of 546 amino acids [7], [8], [9].

More than 170 different mutations are listed in the human gene mutation database. Depending on the type of mutation, its effects on the structure of the mature enzyme and the zygosity, those mutations may lead to G_{M1}-Gangliosidosis in its infantile, juvenile or adult form or to Morquio B disease. The principles of this diversity in development of pathological symptoms still are not fully understood [10].

2.1.2 G_{M1}-Gangliosidosis and MPS IV B

Both GM_1-Gangliosidosis (GM1) and Morquio B disease (MBD) are rare hereditary metabolic disorders with a wide spectrum of both genotypical and phenotypical variety.

Gangliosidoses are a clinically heterogeneous group of inherited neurodegenerative disorders, comprising defects of the metabolism of gangliosides, sialic acid-containing glycosphingolipids. They are caused by a defects of β-galactosidase, β-N-acetylgalactosaminidase, or specific saposins, small proteins needed for the solubilisation and transport of ganglioside substrates in vivo.

The most common form of GM1, termed infantile or type I, is characterized by early onset in infancy and a very limited life span below two years of age. Some cases develop severe cardiomyopathy, which may lead to death before the manifestation of the neurodegenerative character of the disease.

GM1 type II is characterized by a later onset – usually 6 to 36 months – of developmental arrest, followed by regression accompanied by seizures and spasticity. Skeletal abnormalities and macular cherry-red spots, typical symptoms of the juvenile form, are often absent. Death occurs usually in the first decade of life.
Adult forms of GM1 show an even more diverse phenotype, presented by generalized dystonia with dysarthria and ataxia. Cognitive impairment develops later in the course of the disease and life expectancy can range up to several decades after the onset of the disease.
On a cellular level, mutations in the *GLB1* gene leading to GM1 primarily result in the accumulation of G_{M1}-gangliosides within the lysosomal compartment, mainly in the nervous system [10].

Morquio B disease (MBD) – or MPS Type IVB – is classified as a mucopolysaccharidosis, a group of 11 disorders which show defects in different steps of the degradation pathway of glycosaminoglycans, leading to increased storage of these compounds.

In case of MBD, the deficiency of β-galactosidase results in the lysosomal storage of glycosaminoglycans, keratan and chondroitin sulfates, mainly in the lysosomes but also in their secretion via the urinary pathway.
The main symptoms of this disease comprise abnormal skeletal formation, abnormal heart development, hypermobile joints, dwarfism and/or below average height for the certain age of the patient. Neural degeneration or central nervous involvement has not been shown to be part of this disorder [11].

Available evidence indicates that mutations of *GLB1* leading to typical MBD affect the active center of the enzyme while most of the mutations leading to GM1, however, are predominantly found in peripheral areas of the enzyme and thus may interfere with the correct folding of the protein inside the ER. This would affect the transport of β-galactosidase to the lysosomes and is a possible target for enzyme enhancement therapy.

2.1.3 Therapeutic strategies for LSDs

The last two decades have seen a huge increment in research dealing with lysosomal storage disorders as a consequence of the development of novel therapeutic strategies. Furthermore, early biochemical and molecular diagnosis was identified as a pivotal point for appropriate treatment.

So far, none of the novel strategies can entirely replace classical supportive and palliative treatment as well as comprehensive clinical care.

As stated above, the major pathological factor in most LSDs is the abnormal accumulation of distinct enzyme-substrates and substances in cells, tissue and organs. One form of therapy therefore directly aims to inhibit the *de novo* synthesis of enzyme substrates ("substrate reduction therapy" or "substrate restriction therapy"; SRT) and thus diminishes the accumulation of storage material. This allows the residual activity of the degradative enzyme system to handle the newly incoming material for digestion. Accordingly an iminosugar (N-butyldesoxynojirimycin; Miglustat) is currently under approved use for the therapy of Gaucher and Niemann Pick disease type C.

An additional approach seeks to dissolve the accumulated toxic substances within the lysosome and is hence termed "substrate removal therapy". In patients suffering from cysteinosis for instance, thioester linkages are not broken down due to a deficiency of palmitoyl-protein thioesterase. The administration of cysteamine disperses cystine deposits by forming soluble mixed-thiols and also breaks down thioester linkages.

Furthermore, a whole class of therapeutic approaches aims at functional enhancement of deficient enzymes. Beside transplantation of hematopoietic stem cells, the majority of current approaches uses enzyme replacement by infusion of recombinant enzyme every week or every other week. As lysosomal enzymes undergo multiple modifications along trafficking from the ER to the lysosomal compartment, special "high uptake" forms, capable to interact with cell membrane specific receptors (mannose, mannose-6-phosphate and others) have to be used for targeting recombinant enzymes to the lysosome. Currently, ERT preparations are approved for Gaucher disease type I and III, MPS types I, II, IV and VI and are further in clinical development for MPS type IVB, VII and

others.

A major problem of ERT arises from the fact that the central nervous system is inaccessible for supplemented enzymes due to the blood-brain barrier. Current experimental efforts mainly are concentrated to circumvent this restriction by gene replacement or pharmacological chaperone therapy.

Mutant structural genes are supposed to be transferred via a virus-based vector delivery system (gene replacement therapy). Although so far only one preparation has successfully been licensed for clinical application (lipoprotein lipase deficiency (LPLD)), several clinical trials are currently undertaken, e.g. for Sanfilippo syndrome (MPS III). Although therapeutic achievements seem to be promising, the safety aspects of virus-based forms of therapy of therapy have to be observed [11], [12].

Table 1 provides an overview on the principals, advantages and adverse effects of the major therapy approaches to lysosomal diseases (Suzuki et al. [13]).

Table 1: Advantages and limitations of three different therapeutic approaches to lysosomal diseases

	Enzyme replacement	**Substrate reduction**	**Chaperone**
Principle	Enzyme supplementation	Inhibition of substrate synthesis	Enzyme restoration
Administration	Intravenous	Oral	Oral
Target tissue	Extraneural	Neural, Extraneural	Neural, Extraneural
Clinical efficacy	Yes	Yes	Yes
Adverse effect (effective dose)	Yes	Yes	No
Disease specifity	Specific	Nonspecific	Specific
Mutation specifity	Nonspecific	Nonspecific	Specific

2.1.4 Chaperone treatment

Due to the limitations of ERT overcoming the blood-brain barrier small molecules were proposed as possible solution for LSDs like G_{M1}-gangliosidosis which affect the central nervous system.

Pharmacological chaperones (PC) can possibly work on enzyme mutants with aberrant folding, but otherwise fully operational features. According to this concept, the PC, frequently a substrate analog for the enzyme, operates as a competitive inhibitor in vitro, and stabilizes the folding process. Accordingly it can escape the quality control systems in the ER (Endoplasmic-reticulum-associated protein degradation (ERAD)) and can be delivered to the Golgi and further to the lysosomal compartment. As PCs preferably have a higher affinity to their enzymes at a neutral rather than an acidic pH, the natural substrates should mostly displace the PCs once the enzymes reach the lysosome. This may lead to correctly folded, operable enzymes.
The expected advantage of this concept is that due to the molecular character of the chaperone, it can be orally administered and may reach the central nervous system without a block by the blood-brain barrier.

However, this concept requires that the chaperone molecule penetrate the target cell membranes of cells of the primarily affected tissues. PCs can solely work on a selected class of disease associated mutant proteins. Hence, mutant-specific testing is required to confirm the chaperone efficiency. Summing this up, the pharmacological chaperone has to bind to its target enzyme, temporarily stabilize it and then dissociate again once the final destination has been reached.

Currently, several preparations of PCs undergo clinical trial, including drugs to treat Fabry disease, Gaucher disease and Pompe disease [14], [15].

2.1.5 Iminosugars and their derivatives acting as pharmacological chaperones

In contrast to their initial description in the 1960's as anti-viral anti-infective to anti-cancer and anti-diabetes drugs, iminosugars were later discovered as potent glycosidase inhibitors and promising candidates for pharmacological chaperone therapy [16].

1-Deoxygalactonojirimycin, an artificial imino-analogue of galactose [17] acts as a reversible inhibitor of α-galactosidase A and is currently explored in phase III clinical trial for the treatment of Fabry disease [18] under the trading name of migalastat (Amigal). In addition N-alkylated derivatives of 1-deoxynojirimycin were shown to be highly potent

pharmacological chaperones for the treatment of Gaucher and Pompe diseases.

In 2003, the compound N-octyl-4-epi-β-valienamine (NOEV) was described by Suzuki et al. to be an effective inhibitor of human lysosomal β-galactosidase. It was shown that the effective concentration of this substance in culture medium is in the lower nM range. Furthermore, a confirmation of the clinical effectiveness of NOEV has been conducted for G_{M1}-Gangliosidosis model mice, where no clinically recognizable adverse effects had been observed [13].

Wong et al. noted in 2007 that a large lipophilic substituent, linked to the ring-nitrogen of deoxynojirimycin via an alkyl chain with a length from C_3 to C_9, significantly improves interaction with lysosomal glycosphingolipid glucocerebrosidase [19].

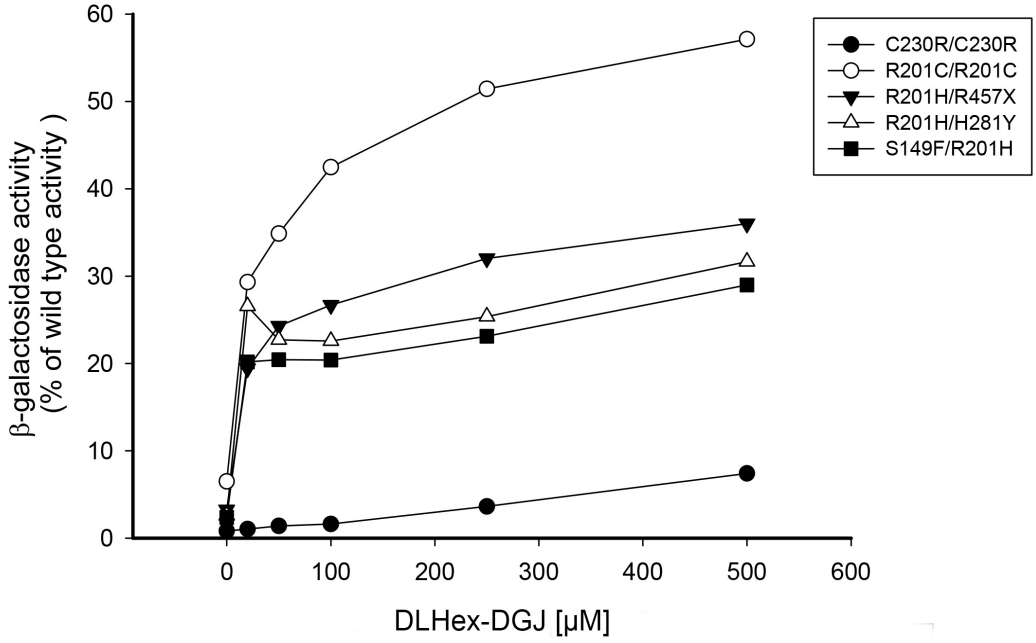

It was described in 2008 by Fantur et al. that 1-deoxy-D-galactonojirimycin-lysine hybrids, synthesized by the Glycogroup of the Department of Organic Chemistry at the Technical University of Graz, are potent D-galactosidase inhibitors which also show activity with human lysosomal β-galactosidase. As the capability of PCs of acting as competitive inhibitors in vitro is crucial for their effectiveness in vivo, K_i and IC_{50} values are of importance. As for DLHex-DGJ – a substance carrying a dansyl moiety – a K_i value of 0,6 µM and an IC_{50} value of 6 µM were reported.

Increased enzyme activity in mutant cell-lines was described, with highest augmentation among the tested substances reported for DLHex-DGJ. Effectiveness was determined by the percentage of enzyme activity restitution in relativity to wild-type levels. To do so, the restoration of β-gal activity was tested on several mutant cell-lines representing both infantile, juvenile and adult forms of GM1 as well as MBD. Best results were achieved for homozygous p.R201C mutants, showing a restitution to 10% wild-type activity – which is commonly considered to be sufficient for normal cellular development – at concentrations of 20 µM of DLHex-DGJ in culture medium. Increment of enzyme-activity continued up to concentrations of 500 µM. A detailed overview of the effects on different mutant enzyme forms can be seen in figure 2 [20], [21].

A novel generation of DGJ-derived PCs, fluorous iminoalditols, were synthesized by the Glycogroup of TU Graz. Subsequent testing of those candidates was carried out in the same manner as for the dansylated compounds. In the known-to-be chaperone sensitive p.R201C mutant, three substances delivered an increase in residual β-galactosidase activity ranging from 35% to 40% of wildtype activity at concentrations ranging from 5 to 50 µM in culture media. Interestingly, however, at distinct higher concentrations of either $(TFM)_3$-OHex-DGJ or $(TFM)_2$-OHex-DGJ in the culture medium, β-galactosidase activity was reported to decrease compared to the most effective concentration [22], [23].

Although most of these substances are characterized in terms of their inhibitory activity in vitro and their activatory potential in vivo, it is still unknown to which proportions the chaperones added to the culture media of cells are actually taken up, in which compartments they accumulate at what concentrations, what are their turnover rates and what influence they exert e.g. on other cellular processes besides the proposed specific catalytic interaction.
Differences between the activatory potential of DLHex-DGJ and fluorinated DGJ-derivates, which show a profound decline of chaperoning at high concentrations in culture medium might be explained by their actually effective intracellular concentrations.

3 Aim

The aim of this master's thesis was to establish a method to detect the molecular chaperone DLHex-DGJ on a Q-Exactive hybrid quadrupole-orbitrap mass spectrometer. The method should be optimized with reference to the ESI-setup in order to produce a preferably high yield of analyte-ions. In parallel, the nature of the drug should be distinctly verified through the analysis of the fragmentation pattern both in positive and negative ion mode. Furthermore, these settings should be adapted to the flow rates of a HPLC-setup. Finally, a practicable extraction procedure of the chaperone from human skin fibroblasts should be established.

With those protocols set up, experiments determining the uptake of DLHex-DGJ in human skin fibroblasts, both in a time- and concentration dependent manner should be conducted, with the final goal of determining both uptake kinetics and subcellular localization of the chaperone and hence contributing to the understanding of the mechanistic background of enzyme enhancement therapy in general.

In a theoretical further approach, the usability of yeast as a model organism in order to study lysosomal storage disorders in general and pharmacological chaperone therapy in particular should be investigated.

4 Material and Methods

4.1 Chromatography and HPLC

Chromatography is a term for a set of techniques with the aim of separating different molecular species from a more or less complex mixture. In order to separate a given molecular species of interest from its co-compounds, a sample is introduced in a flowing mobile phase which passes a stationary phase. Different interactions of molecular species with the stationary phase lead to diverging retention times, with the result of the compounds being separated. The mobile phase can either be a gas (gas chromatography, GC) or a liquid (liquid chromatography, LC). High performance liquid chromatography is a form of liquid chromatography where the liquid mobile phase is pushed trough a column packed with very small porous particles (usually several µm in diameter) which act as solid phase and lead to the separation of an injected sample. Changes in the properties and compositions of stationary and mobile phases hence can be optimized for each compound of interest and the matrix in which it is embedded. The schematic mechanism of the separation is shown in figure 3.

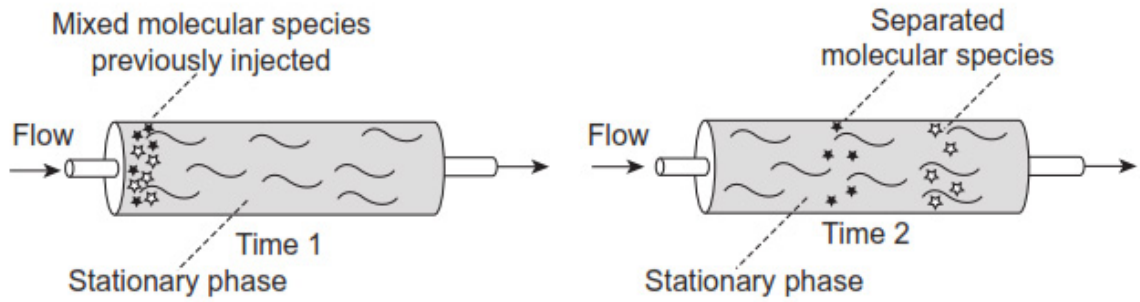

As the mobile phase flows, eluted molecules differ in the time they need to pass the stationary phase, and can be detected after they leave the column (e.g. by UV detectors or mass spectrometers). The graphical output of the generated signal is called chromatogram, where different components are represented by respective peaks at their attributed retention times (t_R) [24].

4.2 Mass spectrometry

The principle of mass spectrometry is to adequately generate ions from organic or inorganic compounds and to separate, detect and specify them according to their mass-to-charge ratio.

Ionization of the compounds can either be achieved through thermic influence, via electromagnetical fields or via the bombardment with energy-rich electrons, ions or photons as well as neutral atoms and the dispersion of electrostatically charged microdroplets. Ions can be either single ionisable atoms, cluster, molecules as well as fragments and associates thereof. Separation of ions usually happens through the influence of statical or dynamical electrical, electromagnetical or electrostatic fields [25].

4.2.1 Electrospray Ionization

In this work, ionization was achieved by the use of a heated electrospray ionization probe, (ESI), where molecules of the sample pass a capillary under a given voltage. In a course of events, the molecules are ionized and separated from the solvent, which happens under the assistance of different streams of nitrogen gas. ESI-ionization is a soft form of ionization which usually yields intact macromolecules. The ions created via electrospray-ionization may be quasi-molecular ions resulting from the addition of a hydrogen cation ($[M+H]^+$), another cation such as sodium ($[M+Na]^+$), a charged solvent molecule ($[M+CO_2H_3]^+$) or the removal of a hydrogen nucleus ($[M-H]^-$). For large macromolecules, multiply charged ions ($[M+nH]^n$) are often observed [25].

4.2.2 Hybrid Quadrupole-Orbitrap

For the consequent mass detection, a hybrid quadrupole-orbitrap mass spectrometer (Q-Exactive, Thermo Scientific©, Bremen) was in use. Advantages of orbitrap mass spectrometers lie in their extraordinary high resolving power combined with the high versatility in fragmentation approaches, which has made them important tools primarily in the field of proteomics, but also a crucial device in many aspects of life sciences, e.g. metabolomics. A schematic setup of a Q-Exactive can be seen in figure 4.

The quadrupole can be used to set up selected reaction monitoring (SIM) experiments, as it acts as a filter which only allows one type of ion with specific m/z to pass through, while all other ions are filtered out. Consequently, working in SIM-mode can significantly increase the yield of target ions.

Ions which have passed the quadrupole are collected in a C-Trap, from where they can be injected to a collision cell to perform fragmentation experiments. For different experimental approaches, in-source fragmentation is an option as well.

The ion-characterization finally takes place in the orbitrap, consisting of a cylindrical outer electrode and a spindle-formed inner electrode, where the ions are injected tangentially and subsequently orbit around the central shaft and alter the electrostatic field, depending on their m/z. This alteration can be translated – through the use of Fourier Transmission – to distinct mass-to-charge ratios with very high accuracy [26].

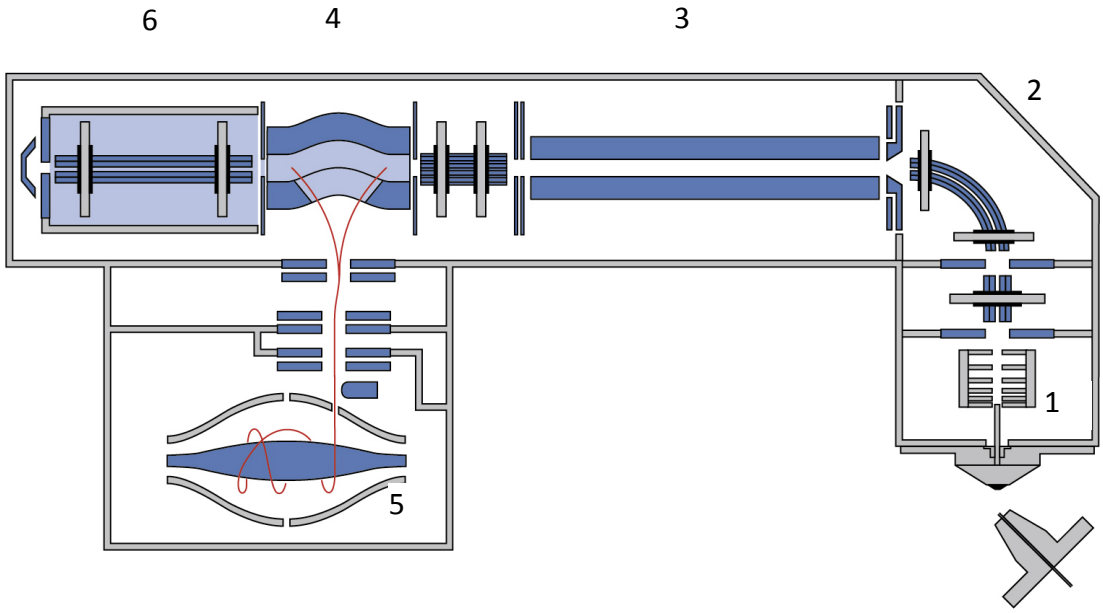

Figure 4: Schematic setup of the Q-Exactive mass spectrometer. Ions, generated at the electrospray ionization source, are transferred via S-lens (1) and ion optics (2) to the quadrupole mass filter (3). After reaching the C-trap (4), the ion current can either be inserted directly into the orbitrap (5) or be passed on to the HCD collision cell (6) first [61].

4.3 Chemicals

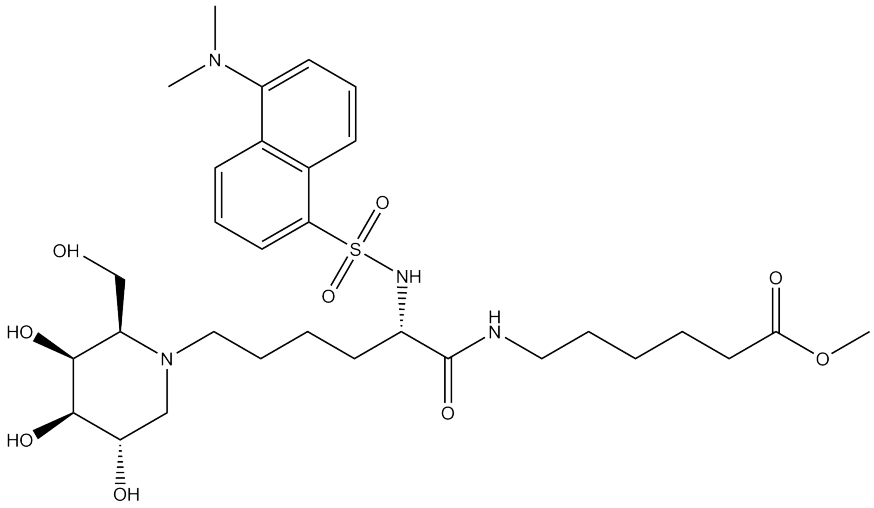

Figure 5: Structure of DLHex-DGJ, generated with ChemDraw Ultra®13 [60].

DLHex-DGJ: Methyl-{[N2-(dansyl)-N6-(1,5-dideoxy-D-galactitol-1,5-diyl)-L-lysyl]amino} hexanoate

The chaperone has been synthesized by the Glycogroup, department of organic chemistry, Technical University of Graz [20].

DLHex-DGJ, provided in form of a dry powder, was dissolved in 100% methanol (EMSURE® Methanol for analysis, Merck KGaA, Darmstadt, Germany). This stock was used for method development procedures, i.e., optimization of ESI conditions, HPLC properties and extraction protocols. As modifier for efficient ion formation in the ESI probe, either acetic acid (EMSURE®, Merck KGaA, Darmstadt, Germany) or formic Acid (EMSURE®, Merck KGaA, Darmstadt, Germany) where used.

Solvents for HPLC-experiments where Methanol (Chromasol V®, gradient grade, for HPLC, Sigma-Aldrich, Steinheim, Germany) and water (Chromasol V®, water for LC-MS, Sigma-Aldrich, Steinheim, Germany), each with 120 µl formic acid and 0,38 g ammonium acetate added to 1 l of solvent, resulting in final concentrations of 0,1% (v/v) formic acid and 5 mM of ammonium acetate.

Lipid extraction was carried out with appropriate compositions of methanol (EMSURE® Methanol for analysis, Merck KGaA, Darmstadt, Germany), chloroform (EMSURE®

Chloroform for analysis, Merck KGaA, Darmstadt, Germany) and deionized water ("Fresenius" Aqua bidest., Fresenius-Kabi, Graz, Austria). Solid phase extraction was done using methanol and water as stated above, with additional use of n-hexane (EMSURE® n-hexane for analysis, Merck KGaA, Darmstadt, Germany).

For fibroblast cultures, Minimal Essential Medium + Earl's salts (Sigma-Aldrich, Steinheim, Germany) was used. 450ml stock solutions of MEM were enriched with 50 ml of fetal calve serum (FCS), resulting in a final concentration of 10 % (v/v) of FCS. Further, 1ml of L-glutamine (29 mg/ml) and 500 µl of gentamicin (50 mg/ml) were added to achieve a final concentration of 400 µM L-glutamine and 50 µg/ml gentamicin.

Determination of enzymatic activity was carried out by the use of 4-methylumbelliferyl β-D-galactoside (Sigma-Aldrich, M-1633), 4-methylumbelliferyl-N-ecetyl β-D-glucosaminid (Sigma Aldrich; M-2133), Natriumacetat-2-hydrate (Merck; 6448), citric acid (Merck; 244), sodium chloride (Merck; 1.06404) and sodium azide (Merck; 6688), bovine serum albumine (Sigma-Aldrich, A-3912), glycine (Roth; 3908.2) and sodium hydroxide (Merck; 6498).

4.4 Preparation of stock solutions

For method development purposes, a stock solution of the chaperone was prepared by dissolving 4,56 mg of DLHex-DGJ in 9,02 ml of methanol, resulting in a concentration of 500 µg/ml. The stock solution was stored dark at -18°C.

Dilutions of this stock where made using methanol with the addition of approximately 0,1% of either formic acid or acetic acid as modifier for the ionization.
Furthermore, dilutions for the HPLC where made using a mixture of 50% methanol and 50% aqua dest. and again 0,1% of formic acid as modifier.

For the application to fibroblasts given amounts of DLHex-DGJ were dissolved in PhoBI buffer in a final concentration of 10 mg/ml (Table 2).

Table 2: Composition of PhoBI buffer prepared for application of DLHex-DGJ

Phosphate buffer; pH 7,0	10 mM
NaCl	100 mM

Triton X-100	0,01 % (v/v)

4.5 Cell culture

Cell lines from two different patients were in use: Cell line A, derived from a healthy patient ("wild type"), and cell line B, derived from a patient with juvenile G_{M1}-gangliosidosis carrying a homozygous mutation, p.R201C, in exon 6 of its *GLB1* gene which is known to be chaperone-sensitive ("mutant cell line").

Unless otherwise stated, human skin fibroblasts where grown seven days at 37°C and 5% CO_2 until becoming confluent and being either split to further flasks or harvested for analysis. After three to four days of growth, the medium was removed and fresh medium added.

Cells grown for method optimization or western blot analysis were grown in 75 cm^2 flasks. Experiments on uptake kinetics were carried out using 6-well plates (9.5cm^2). For digitonin-treatment 25 cm^2 flasks were used.

Composition of the growth medium can be found in chapter 4.3.
All work which required a sterile environment was conducted using a Kendro HeraSafe® laminar flow box.
Cells were incubated at given conditions in a CO_2-Incubator (Fisher Scientific Isotemp®).

4.5.1 Chaperone application

For long term uptake experiments, lasting up to 96h, the chaperone was added to subcultured cells after 3 days of growth, alongside with the regular addition of fresh culture medium.

For short-term uptake experiments, culture medium was changed regularly after three days, while addition of the chaperone was done on the sixth day of the subcultures with an additional change of culture medium. This was done in order to normalize growth conditions for different time points of the experiment.

For either of the protocols, calculated amounts of PhoBI-dissolved DLHex-DGJ were added

to the culture medium and sterile filtrated using 0,12 µM filters immediately before application.

4.5.2 Subcultivation

Subcultivation of confluent cell culture flasks was carried out according to table 3.

*Table 3: **Subcultivation of fibroblasts with 1/3 Splitting.** Other splitting proportions have been achieved by changing the amount of medium for resuspension after the centrifugation step*

	75 cm² Flask	**25 cm² Flask**
Grow cells until they become confluent		
Remove medium		
Wash twice with PBS	6 ml	4 ml
Add Trypsin	4 ml	2 ml
Incubate for 3 min at 37°C		
Stop digestion by adding fresh medium	4 ml	2 ml
Wash off cells with medium and transfer to centrifuge tube	4 ml	2 ml
Centrifugation for 2 min at 2500 rpm		
Remove supernatant		
Resuspend cells well in fresh medium	9 ml	3 ml
Prepare fresh flasks by adding medium	12 ml	6 ml
Transfer cells to new flasks	3 ml	1 ml

When 6-well plates were used, 2,5 ml of growth medium were dispensed to each well and 0,5 ml of cell suspension were added to a total amount of 3 ml. With this protocol, it was possible to inoculate three 6-well plates with the use of one 75 cm² flask grown to confluency.

Confluent cells in 6-well plates were never used for further subcultivation steps.

4.5.3 Harvesting

Depending on the further application, three different protocols were in use for harvesting confluent cell layer.

Protocol A was used for method optimization as well as for western blot utilization (Table 4).

Table 4: ***Protocol A, non-sterile harvesting of fibroblasts***

	75 cm² Flask	**25 cm² Flask**
Grow cells until they become confluent		
Remove medium		
Add Trypsin (non sterile)	4 ml	2 ml
Incubate for 3 min at 37°C		
Stop digestion by adding physiological saline solution (non sterile)	4 ml	2 ml
Wash off remaining cells with physiological saline solution	4 ml	2 ml
Transfer cell suspension to a 15 ml Greiner tube		
Centrifuge for 2 min at 2500 rpm		
Remove supernatant		
Resuspend pellet in physiological saline solution and vortex briefly	6 ml	4 ml
Centrifuge for 2 min at 2500 rpm		
Remove supernatant		
Store dry pellet at -20°C		

Protocol B was used for cells grown in 6-well plates to be used for uptake kinetics and enzyme activity (table 5).

Table 5: ***Protocol B; non-sterile harvesting of fibroblasts from 6-well plates****; All quantities refer to one single well*

	6-well plates
Grow cells until they become confluent	
Remove medium	
Add physiological saline solution	5 ml
Wash cells by gentle agitation	
Remove supernatant	
Add physiological saline solution	5 ml
Wash cells by gentle agitation	
Remove supernatant	

Add physiological saline solution	100 µl
Thoroughly scrape off cells using a cell scraper	
Wash off cells from cell scraper using physiological saline solution	100 µl
Transfer cell suspension to Eppendorf tube	
Store at -20°C	

Protocol C was used for cells grown for further digitonin treatment in 25 cm² flasks (table 6).

Table 6: ***Protocol C; non-sterile harvesting of fibroblasts from 25 cm² flasks*** *for further digitonin treatment*

	25 cm² flask
Grow cells until they become confluent	
Remove medium	
Add trypsin (non sterile)	2 ml
Incubate for 10 min at room temperature without agitation	
Stop digestion by adding physiologic saline solution	2 ml
Wash off remaining cells with physiological saline solution	2 ml
Transfer cell suspension to a 15 ml Greiner tube	
Centrifuge for 2 min at 2500 rpm	
Remove supernatant	
Thoroughly scrape off cells using a cell scraper	
Resuspend pellet in physiologic saline solution and vortex briefly	2 ml
Centrifuge for 2 min at 2500 rpm	
Remove supernatant	
Store at -20°C	

4.6 Lipid extraction

In order to analyze the amount of chaperone uptake by cells, an extraction step had to be included, in order to protect the HPLC and mass spectrometry equipment.

Extraction was based on some modifications of the standard Bligh and Dyer extraction procedure. The final extraction protocol can be seen in table 7, while the details of

method development are described in chapter 5.1.4.

Table 7: Final and optimized protocol for the extraction of DLHex-DGJ from harvested fibroblasts

Lipid extraction protocol
resuspend harvested cells in 1 ml aqua dest.
add 5 ml chloroform/methanol (2:1)
vortex for 1 min
ventrifuge for 8 min @ 2500 rpm
remove organic phase and set aside
add 4 ml chloroform/methanol (5:1) to remaining aqueous phase
vortex for 30 seconds
centrifuge for 8 min @ 2500 rpm
remove organic phase and reunite with organic phase from previous step
add 4 ml chloroform/methanol (5:1) to remaining aqueous phase
vortex for 30 seconds
ventrifuge for 8 min @ 2500 rpm
remove organic phase and reunite with organic phase from previous step
evaporate under nitrogen stream
resuspend in desired solvent

In cases where the cells were already dissolved, the amount of water in the first extraction step was reduced to yield a final volume of 1 ml.

4.7 Solid phase extraction

As extracts resulting from Bligh-Dyer procedure required further purification before being applied to the HPLC equipment a solid phase extraction step was added.

Solid phase columns (Agilent® C18 SPE cartridges) were used. All SPE steps were carried out using an Agilent® vacuum manifold attached to an aspirator pump. Protocol optimization can be seen in detail in chapter 5.1.5, while the final protocol is observable in table 8.

Table 8: Final protocol for the clean-up of lipid extracts via SPE

Solid Phase Extraction protocol	
Sample pre-treatment:	resuspend sample in 100 µl of a 1/1 methanol/water-mixture
Column conditioning:	4ml methanol
	4 ml water
Loading:	100 µl of sample
Washing step I:	4 ml aqua dest.
	let column run dry for 5 min
Washing step II:	4 ml n-hexane
	let column run dry for 10 min
Elution:	4 ml methanol/water (6/1)
Sample post-treatment:	evaporate solvent under nitrogen stream
	resuspend in desired amount of solvent

4.8 Western Blot

Cells were harvested according to the protocol in chapter 4.5.3. Pellets were resuspended in 500µl of Solution A (0,9% NaCl, 0,1% Triton X-100) and the pellets of two flasks, handled in duplicate up to that point, were pooled. Cells were disrupted with a Branson® Sonifier 250 ultrasonic benchtop system, in continuous mode at a sonication intensity of approximately 20 mV. Cell suspensions were precooled in an ice bath and sonicated twice over a period of 10 seconds, with 30 seconds of cooling time in-between. After a centrifugation step of 30 seconds at 10,000 rpm, total cell protein was determined, using the protocol given in chapter 4.9.

Samples were subsequently diluted to a protein concentration of 20 µg and 30 µg in 12 µl, respectively. After addition of 3 µl of sample buffer and 1 µl of reducing agent to each specimen, samples were denatured for 10 minutes at 70°C under continuous shaking. Proteins were then subjected to SDS-PAGE, using 10% Tris-HCl ready-made gels with 1mm of strength (Bio-Rad, Hercules, CA). SeeBlue® Plus2 pre-stained protein ladder (LC5925, Invitrogen) was used as standard. Separated proteins were transferred to Immobilin-P PDVD membranes with 0,45µM pore size. Blotting was performed at 300 mA for 90 minutes.

Thereafter, membranes were blocked using 10 ml of 5% dry milk, dissolved in Tris-buffered saline with tween20 (TBS-T) for 45 minutes. Primary and secondary antibodies were diluted in 5% dry milk in TBS.

To visualize human β-galactosidase in the whole cell lysates, a rabbit polyclonal anti-β-GAL antibody (1:50, ZAT0810) was used as described by Fantur et al. [21].

Incubation with the primary antibody was done overnight at 4°C. After removal of the primary antibody, the membrane was immediately rinsed shortly for three times with TBS-T and then further washed for three times under incubation with TBS-T for 5 minutes. Incubation with the secondary antibody, alkaline phosphatase coupled anti-rabbit IgG (1:20 000, Sigma Aldrich, Taufkirchen, Germany), was done for 1 hour. After using the same washing procedure as above, protein bands were visualized with a Western Blot Detection Kit (Bio-Rad, Hercules, CA). After the color-forming reaction was completed, membranes were dried and scanned for further analysis.

4.9 Protein determination

Determination of protein concentration was done according to Lowry et al. Cells were homogenized using a Branson© Sonifier 250 ultrasonic bench-top system. Cell suspensions were put in an ice bath and sonicated twice for 10 seconds, with 30 seconds of cooling time in-between. Ultrasonicator was set to continuous mode with an output of approximately 20 mV. Protein was measured in duplicates by adding 20 µl of cell homogenate to 20 µl of 20 % NaOH, using deionized water for blank measurements. 40µl of BSA with a concentration of 1 mg/ml, dissolved in 10% NaOH, were used as a standard.

After addition of 60 µl of 2N acetic acid to each sample, 1 ml of alkaline $CuSO_4$ solution was added with immediate agitation. Samples were then incubated for 10 minutes at room temperature. Color-forming reaction was started with the addition of 100 µl Follin reagent (1:3 dilution in deionized water) and extinction at 623 nm was determined after an incubation time of 10 minutes. (Shimadzu© UV-1800 Photometer).

For calculation, the extinction of blanks was subtracted from sample extinctions and protein concentration was calculated using extinction of the BSA-samples as standard.

4.10 Determination of enzyme activity

The effectiveness of molecular chaperones is estimated by determining the increase of mutant target enzyme in cells cultured in the presence of chaperone. This is accomplished by measuring the activity of β-galactosidase as the target activity and β-hexosaminidase as an internal control for specificity. Activities were measured by determining the increase of fluorescence at alkaline pH caused by the release of 4-methylumbelliferone from the 4-methylumbelliferyl(4-MU)-ß-D-galactoside or 4-MU-ß-D-N-acetylgalactosaminide respectively. As free 4-MU, but not its substrate-linked form, shows a characteristic excitation at a wavelength of 365 nm in mildly basic environment its fluorescence can be used to determine the amount of degraded substrate during a given period of time and to calculate the specific enzyme activity in nmol/hour and mg isolated protein.

4.10.1 β-Galactosidase

Activity of β-galactosidase was determined in order to find a correlation between the kinetics of the uptake of DLHex-DGJ and its ability to restore the enzymatic function of β-galactosidase.
Buffers and solutions in use can be found in table 9.

Table 9: List of substrates and solutions used for enzyme activity determination of β-galactosidase

Substrate	0,5 mM 4MU-β-D-galactoside in substrate buffer
Substrate buffer	100 mM sodium citrate buffer, 0,02% sodium azide; pH 4,0
Stop buffer	0,4 M Glycin/NaOH; pH 10,4

Before determination of the enzymatic activity, cells had to be homogenized and the amount of cellular protein had to be determined according to the protocol given in chapter 4.9.

Every sample was measured in duplicate, alongside with a third measurement of the sample without addition of substrate, hence indicating an enzyme blank (EB). Two substrate blanks were prepared for every experiment. Detailed composition of the

experimental preparation can be found in table 10.

Table 10: Composition of β-GAL determination mixtures; Incubation time was 30 min at 37°C

Substrate blank (SB)	20 µl	0,9% NaCl + 0,01% Triton X100
	100µl	Substrate
Enzyme blank (EB)	20 µl	Cell homogenate
	100 µl	Substrate buffer
Sample	20 µl	Cell homogenate
	100 µl	Substrate

After incubation for 30 minutes at 37°C, the reaction was stopped by the addition of 2,5 ml of stop buffer.

Fluorimeter in use was Perkin Elmer© LS50B, excitation wavelength was set to 360 nm, emission wavelength to 450 nm. Sipping time was set to 3, fluorimeter cell was flushed with distilled water before and after every batch of samples.

A solution of 0,08 mM 4-methylumbelliferone in stop buffer was prepared before every experiment for calibration.
Factor ΔF was calculated as mean value of the sample minus substrate blank and enzyme blank.

Calculation of factor f was done according to the following formula given in figure 6.

$$f = \frac{C_{st} * V}{F_{st} * t * v}$$

Figure 6: Calculation of factor f where C_{st} is the concentration of the calibration solution (µmol/l), V is the volume of the sample (µl), F_{st} is the measured value of the calibration solution (arbitrary), t is incubation time (min) and v is volume of cell homogenate in sample (µl)

Enzymatic activity is calculated as f* ΔF = nmol/h for non-diluted samples.

4.10.2 β-Hexosaminidase

In experiments where β-galactosidase activity was measured, activity of β-hexosaminidase was determined as normalization factor. In experiments involving digitonin, β-

hexosaminidase activity was measured in order to monitor release of the lysosomal fraction.

Buffers and solutions in use can be found in table 11.

Table 11: List of substrates and solutions used for enzyme activity determination of β-hexosaminidase

Substrate	1 mM 4MU-N-acetyl-β-D-glucosaminide; in substrate buffer
Substrate buffer	100 mM sodium citrate buffer, 0,2% BSA, 0,02% sodium azide; pH 4,0
Stop buffer	0,4 M Glycin/NaOH; pH 10,4

Before determination of the enzymatic activity, cells had to be homogenized and amount of cellular protein had to be determined according to the protocol given in chapter 4.9.

Tenfold dilution of every sample was prepared and measured in a duplicate way, alongside with a third measurement of the sample without addition of substrate, hence indicating an enzyme blank (EB). Two substrate blanks were prepared for every experiment. Detailed composition of the experimental preparation can be found in table 12.

Table 12: Composition of b-HEX determination mixtures; Incubation time was 10 or 15 min at 37°C

Substrate blank (SB)	10 µl	0,9% NaCl + 0,01% Triton X100
	90 µl	0,9% NaCl
	100µl	Substrate
Enzyme blank (EB)	10 µl	Cell homogenate
	90 µl	0,9% NaCl
	100 µl	Substrate buffer
Sample	10 µl	Cell homogenate
	90 µl	0,9% NaCl
	100 µl	Substrate

After incubation for 10 minutes at 37°C, the reaction was stopped by the addition of 2,5

ml of stop buffer.
Detection and calculation of enzyme activity were done according to the protocol given in chapter 4.10.1.

4.11 Digitonin treatment

Cells were harvested according to the protocol specified for digitonin treatment given in chapter 4.5.3. Pellet was resuspended in 800 µl of digitonin solution (0,25M Succrose; 10mM Tris pH 7.0; 50 µg/ml digitonin).

Digitonin had to be cleaned according to the protocol of Janski et al [27] prior to application.
After incubation for 10 minutes on ice, 400 µl were set aside and labelled whole-cell suspension for later use. Remaining 400 µl were centrifuged for 10 minutes with 9000 rpm at 4°C. Supernatant, containing primarily cytoplasmic components, was set aside. The remaining pellet, comprising cell membrane fragments and organelles, was resuspended in 400 µl of succrose solution (0,25M Succrose; 10mM Tris pH 7.0).

Subsequent determinations of enzyme activity and chaperone concentration were done immediately for those fractions.

4.12 Quantitation of DLHEx-DGJ in cell homogenates and culture medium

4.12.1 Equipment

Mass spectrometry experiments were performed with a Thermo Scientific© Q-Exactive hybrid quadrupole-orbitrap mass spectrometer.
Direct injections with concentrated samples were done using an automated syringe drive along with a 500 µl Hamilton syringe.
For chromatographic separation prior to mass spectrometry analysis, a Thermo Scientific HPLC system equipped with two Accela 1250 pumps and connected to a Thermo Scientific AutoSampler were used. Samples were injected from a cooled repository. Column selection was directed via a Maylab MistraSwitch heated column oven, which facilitates the use of up to six columns in parallel. Sample ionization finally came to pass in an ESI II

heated probe, from where generated ions entered the mass spectrometer.

Via the use of a separate valve, intercalated between the column oven and the ESI probe, it was possible to deflected undesirable fractions from the HPLC column and directly route them to a waste bin, which prevents the mass spectrometer from premature and superfluous contamination.

4.12.2 MS optimization

In order to optimize the conditions of the ESI probe and the subsequent mass detection, different dilutions of the chaperone-solution were injected directly into the ion source, using a Hamilton 500 µl syringe. The syringe driver was set to a flow-rate of 5 µl/min.

The initial settings of the ESI probe were set according to the recommendation of the Thermo Scientific user guide corresponding to the flow-rate, as can be seen in table 13.

Table 13: Initial heated electrospray settings as recommended by Thermo Scientific for a flow rate of 5 µl/min in positive and negative ion mode respectively

Sheath gas pressure (psi)	5
Auxilliary gas flow (arbitrary units)	0
Sweep gas flow (arbitrary units)	0
Ion transfer tube temperature (°C)	240
H-ESI vaporizer temperature (°C)	50
Spray voltage (V)	+3000 / -2500

Subsequently, each parameter of the ESI was step-by-step optimized in order to maximize the yield of molecule-ions.

During this part of the experiment, the mass range was set to 100-1500 m/z so that also possible fragments and adduct-complexes of the chaperone could be detected.
Initial optimization procedures were done using formic acid at a concentration of approximately 0,1 to 0,5 % (v/v). Modifiers were used both for positive and negative ion mode- ESI in order to facilitate the protonation and deprotonation respectively.
In accordance to a publication of Wu et al. in 2004 [28], acetic acid was compared to formic acid as modifier, in an approach to potentially amplify ion yield in parallel with ESI optimization.

After roughly setting the parameters of the ESI via direct injection, given dilutions of the chaperone where transferred into vials and placed into the cooled repository of the Accela Open AS Autosampler (Thermo Scientific, Bremen). Subsequently, a by-pass tube was placed in the column oven to optimize the settings of the ESI probe for the higher flow-rates of the HPLC system, but without the time-consuming interconnection of a HPLC column. ESI-settings were optimized for flow-rates of 200 µl/min and 300 µl/min respectively.

4.12.3 MS/MS analysis

DLHex-DGJ had initially to be characterized for its exact mass and fragmentation pattern. For this purpose, the quadrupole mass filter was set to a range of 651,3 +/- 0,4 m/z in negative mode and 653,3 +/- 0,4 m/z respectively. If a given threshold of ions is reached, the C-trap releases the ion-package to the HCD collision cell and subsequently generated daughter-ions are measured via the orbitrap.

The collision energy in the HCD collision cell (given in % of maximal collision energy) was set both in positive and negative ion mode to optimize the yield of daughter ions. Furthermore, associated settings in Q-Exactive Tandem-MS mode such as ion threshold, under-fill ratio and dynamic exclusion were optimized in a way that fragmentation does not affect the consequent quantification of the parent ion.

Up to this point, experiments were carried out both in positive and negative ion mode. After evaluation of the resulting mass spectra, the negative ion-mode turned out to be more favorable since more of the generated fragments could be assigned with distinct fragmentation patterns.

4.12.4 HPLC separation

To detect the chaperone amongst the complex matrix of fibroblast extracts, a chromatography method had to be set up to separate the substance from other contaminants.

Due to the rather hydrophobic character of DLHex-DGJ, caused by both its lysine and hexanoate moiety, a reversed-phase column (Hypersil Gold 50 x 2,1 mm C18 column with

3 µm bead-size) was chosen. As mobile phase, varying ratios of methanol (HPLC-grade, Sigma-Aldrich, Steinheim) and water (HPLC-grade, Sigma-Aldrich, Steinheim), each with addition of 0,12 % formic acid and 5 mM ammonium acetate, were used.

Starting conditions were set according to general recommendations for this kind of separation, including a relatively low flow rate (200 µl/min), a mobile phase composition of 100 % methanol, and a total runtime of 25 minutes. For initial optimization steps, samples of DLHex-DGJ were used at concentrations proven to be feasible in prior ESI optimization steps without the addition of any matrix components. The injection volume was set to 10 µl. With given starting conditions, retention time of the DLHex-DGJ appeared to be about 0,6 minutes, which essentially indicated no significant retention at the column at all, as the same elution time was observed for the eluent itself to pass the column.

Consequently, the composition of the mobile phase was optimized for an appropriate retention time without affecting the peak shape in terms of broadening or double-peaking. This was done by consecutive addition of water to the mobile phase. At a composition of 50 % methanol and 50 % water, the retention time of DLHex-DGJ was found to be at 2,0 minutes, which was considered acceptable for the substance to be separated from more lipophilic components, supposed to elute later, as well as from more polar particles, poorly detained by the column and therefore expected to elute earlier.

As soon as appropriate conditions were found, the flow rate could be increased to 300 µl to shorten the runtime and improve the efficiency of the method without affecting the chromatographic parameters.

For removal of further non-polar elements, the composition of the mobile phase was switched from isocratic to a gradient method with increasing amount of methanol. This had to be done to clean the column and to avoid carry-overs to succeeding runs.

To finally equilibrate the column for the next run, ending conditions had to be the same as the staring conditions. The final composition of the mobile phase can be found in table 14.

Table 14: Final composition of mobile phases for the HPLC protocol; Mobile Phase A was methanol, Mobile Phase B was water; both with the addition of 120 µl of formic acid and 0,38 g of ammonium acetate per liter respectively

Minutes	Gradient % solution A/B	Flow-rate (µl/min)
0:00	50-50	300
2:36	50-50	300
4:00	100-0	300
11:00	100-0	300
13:00	50-50	300
16:00	50-50	300

4.12.5 Calibration and evaluation

In the course of optimizing extraction and cleaning protocols, it became necessary to evaluate the efficiency of the developmental steps. Above all, this was inevitable as no internal standard was available, making external calibration the only tool to sufficiently quantify the chaperone. Consequently, a calibration curve was compiled solely for optimization of extraction methods. Further optimization of lipid extraction and solid phase extraction protocols were evaluated with reference to this calibration curve.

Evaluation of the method further included determination of both limit of detection (LOD) and limit of quantification (LOQ) for the HPLC-MS part alone, as well as the detection limit for the complete extraction procedure, termed MDL (method detection limit). Calculation was done by comparison of the signal peak height to background noise. According to common conception, limit for LOQ was set at a signal-to-noise ratio of 10 to 1, while the limit for LOD was set to a ratio of 3:1.

Absence of an internal standard was considered to render the quantification procedure prone to both random and systemic errors. For this reason, additional calibration samples were prepared which were subjected to the same optimized extraction steps every routine sample had to undergo. This ensured the absence of systemic errors for the extraction protocol. It was further decided to inject all routinely extracted samples in batch with the calibration samples to the HPLC-MS device. With this procedure, intra-day

variations of the mass spectrometry device could be eliminated.

4.12.5.1 Calibration curves

The optimized method for the detection was used and performed as previously described in order to generate a calibration curve for DLHex-DGJ. This was done by trifold measurements of eight given concentrations.

The peak area of the extracted ion current (XIC) of DLHex-DGJ (m/z 651,3067 +/- 6 ppm) was determined automatically using Genesis detection algorithm of Thermo Scientific Xcalibur© software.

The obtained data was outlined with respect to the given concentration. Thereof, a trendline was generated using the Microsoft Excel 2003© software. The graph, along with error bars an trendline-equation, can be seen in figure 7.

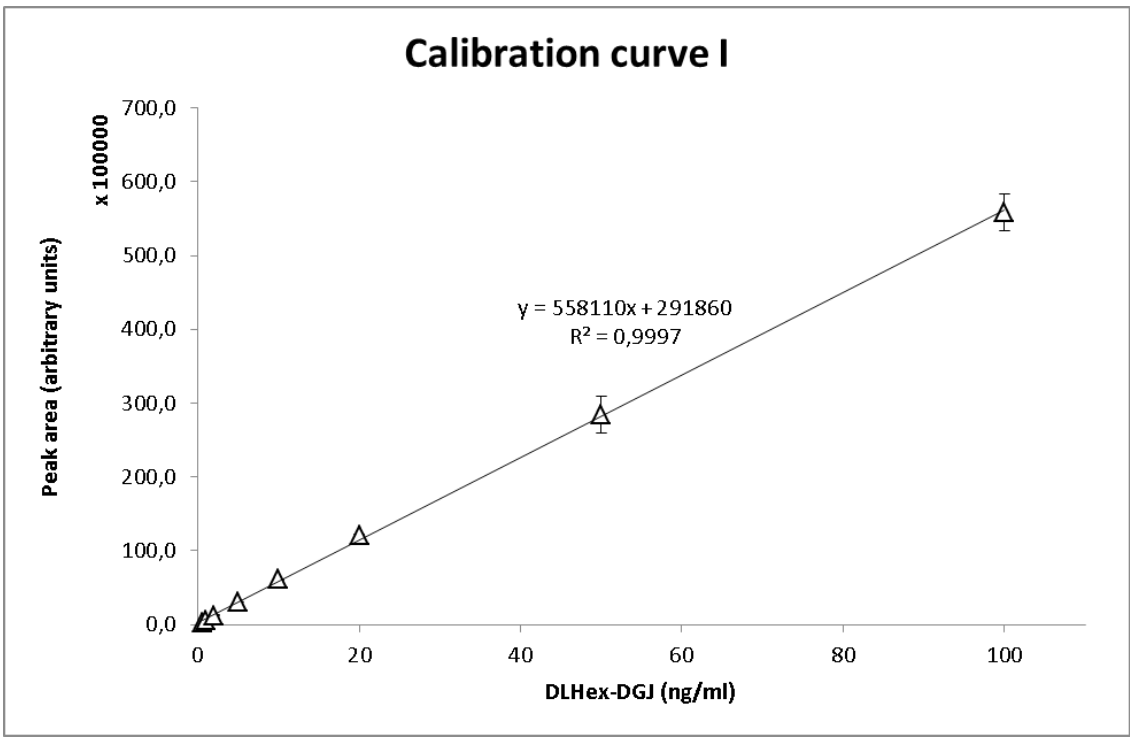

Figure 7: Calibration curve generated by trifold measurement of different dilutions of DLHex-DGJ

4.12.5.2 Limit of detection (LOD) and limit of quantification (LOQ)

Calculation was done based on the correlation of signal peak height to background noise.

For this approach, several dilutions of DLHex-DGJ were prepared and measured via the HPLC-MS device. This was done concordantly for determination of MDL were prepared samples were also subjected to the different extraction protocols.

For those samples yielding appropriate signal to noise ratios near LOD and LOQ, dilutions were prepared two more times and measured thereupon. Mean values for the resulting triplicate measurements were calculated and used to generate a calibration curve. Linear equation thereof was determined and finally used to calculate LOD, LOQ and MDL respectively.

5 Results

5.1 Method optimization

5.1.1 Detection of DLHex-DGJ

For the first detection experiments, a 1/10 dilution of the stock-solution, resulting in a final concentration of 100 µg/ml, had been prepared, using methanol without any additional modifiers. The injection into the ESI probe was carried out using the syringe driver at a flow rate of 5 µl/min. The mass range of the orbitrap was set to a region between 100 m/z and 1500 m/z and a resolution of 140 000 in order to detect possible fragments or adducts. The quadrupole mass filter was not in use. No signal of the chaperone at its distinct m/z ratio of 651,3 in negative mode or 653,3 in positive mode was detected. Settings of the ESI were left at default for the flow rate, as recommended by Thermo Scientific.

Assuming that too high concentrations may result in inhibition of signal, further dilutions were prepared. Thus, it was possible to detect the chaperone both in negative and positive ion mode at concentrations of 5 µg/ml as well as 500 ng/ml and 100 ng/ml at standard conditions and with the addition of formic acid.

Forms of quasi-molecular ions that could have been identified comprised mainly $[M+H]^+$ with an m/z of 653,3220 in positive ion mode and $[M-H]^-$ with an m/z of 651,3064 in negative ion mode. Formation of ions with components of the solvent were barely detectable. $[M+Na]^+$ (m/z 675,3040) in positive mode and $[M+FA]^-$ (m/z 697,3040) in negative ion mode showed an abundance of less than 10% with respect to the hydrogen adducts. An overview of the detectable ion-forms of DLHex-DGJ can be found in figure 8.

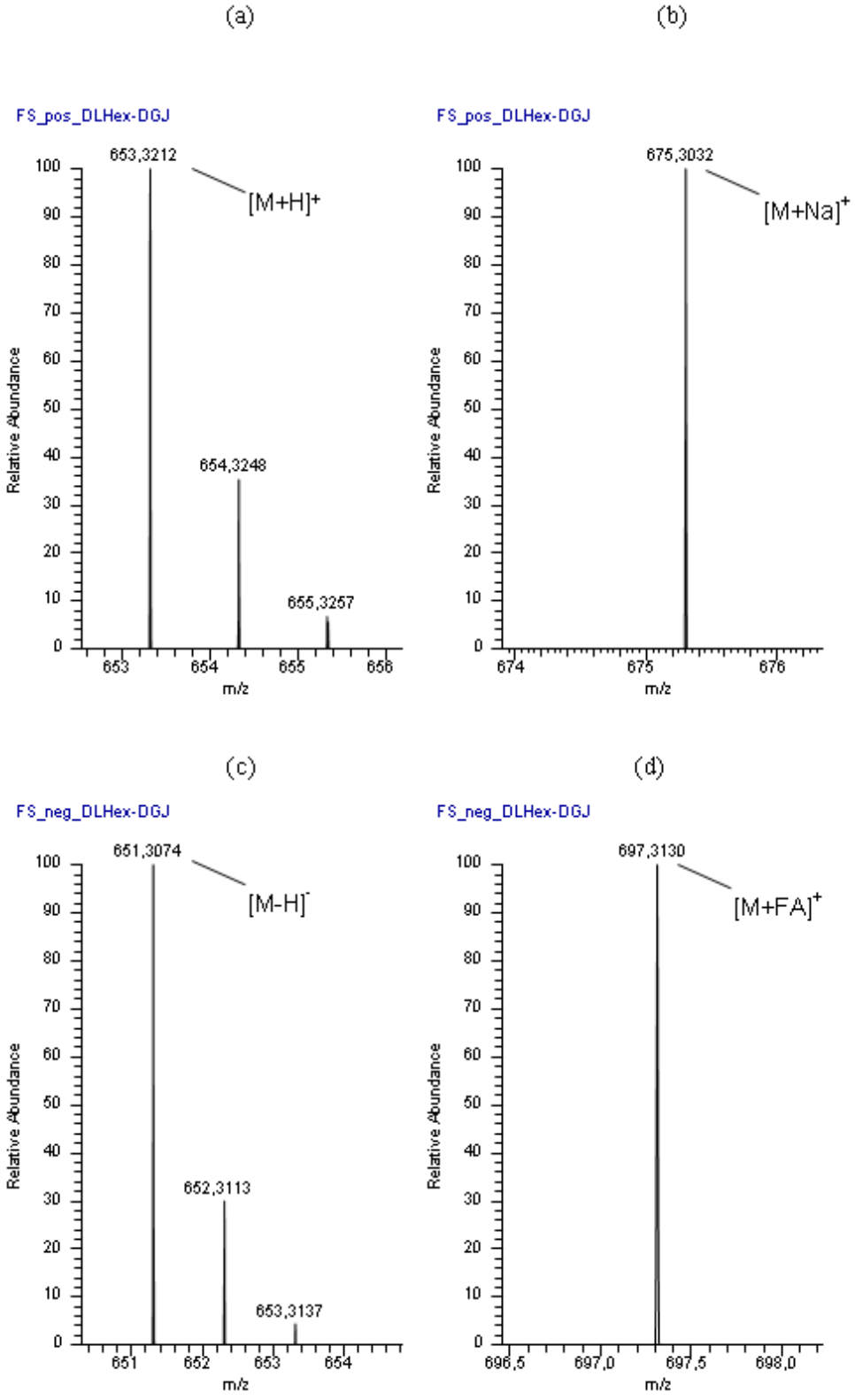

By changing the parameters one by one during injection, preliminary settings had been found in which the ion yield at the destined mass was at maximum. The settings are summarized in table 15.

Table 15: Preliminary optimization of H-ESI settings for flow rate of 5 µl/min and concentrations of 100 ng/ml to 5 µg/ml. Data is shown for both positive and negative ion mode

Sheath gas pressure (psi)	15 (+) / 10 (-)
Auxiliary gas flow (arbitrary units)	5 (+) / 0 (-)
Sweep gas flow (arbitrary units)	0 (+/-)
Ion transfer tube temperature (°C)	280 (+/-)
H-ESI vaporizer temperature (°C)	80 (+) / 50 (-)
Spray voltage (V)	+ 3600 / - 5000

As can be found in literature, the addition of weak acids as modifier in negative-ion electrospray ionization MS may lead to a higher yield of ions [28]. Therefore, in the same experimental setup, the addition of acetic acid instead of formic acid as modifier was tested by adding approximately 0,1% acetic acid to the samples. Results can be seen in figure 9, where the highest intensities of the XIC at 651,3 m/z +/- 6ppm in negative-mode and 653,3 m/z +/- 6ppm in positive mode are outlined.

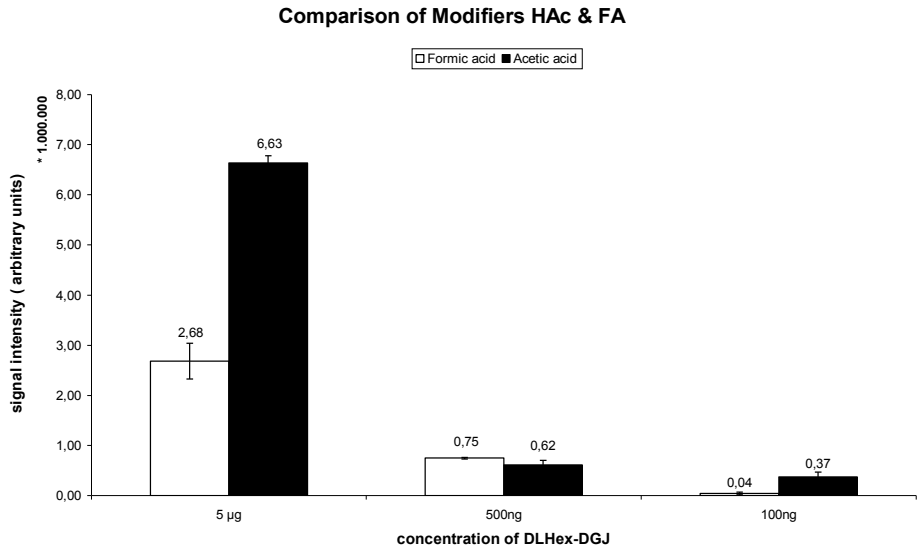

Figure 9: Comparison of the signal intensity of triplicate measurements with different modifiers and chaperone concentrations

Figure 10 shows the comparison of positive and negative ion mode in matters of total yield of target ions for different concentrations and modifiers.

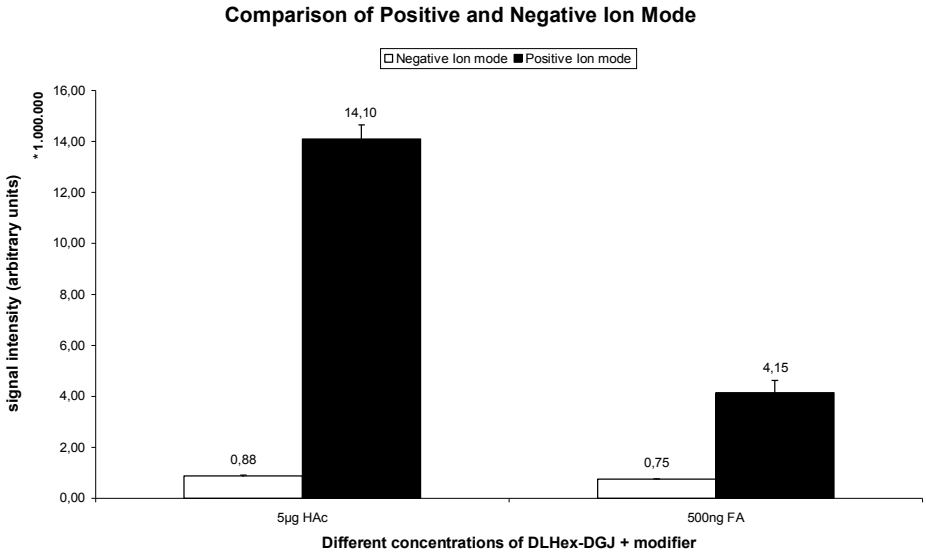

As can be seen in figure 9 and 10 the total yield of ions was higher when using acetic acid instead of formic acid. Furthermore, the obtained signal was significantly higher in positive ion mode compared to negative ion mode.

In contrast to these findings, the further measurements and optimizations where carried out in negative ion mode and with formic acid as modifier. The reasons for this are as follows: as for the modifier, the number of solvents to be used on the HPLC installation is limited to four, whereof one was loaded with methanol and formic acid by other members of the laboratory and the other three were used for water, acetonitril and a mixture of both respectively. Since a constant change of solvent between the runs was considered too time-consuming, it was decided to use formic acid as modifier instead of acetic acid. The reasons why negative ion mode was chosen over positive ion mode are explained in chapter 6.1.

5.1.2 Fragmentation

Since it was considered necessary to characterize the chaperone not only by high accuracy molecular weight determination, but also by finding a distinct fragmentation pattern, tandem-MS experiments have been carried out.

For this reason, the quadrupole mass filter was set to an isolation window of 651,3 +/- 0,4 m/z in negative ion mode and 653,3 +/- 0,4 m/z in positive ion mode.

Passing ions where detected in the orbitrap and, once reaching a given threshold, sent to

the HCD collision cell, where fragmentation with a given collision energy was carried out. The generated fragments where sent back via the C-trap to the orbitrap in order to characterize the fragmentation pattern. All of the above steps are executed automatically by the Thermo Scientific software.

Fragmentation in positive ion mode lead to a distribution of daughter ions as seen in figure 11.

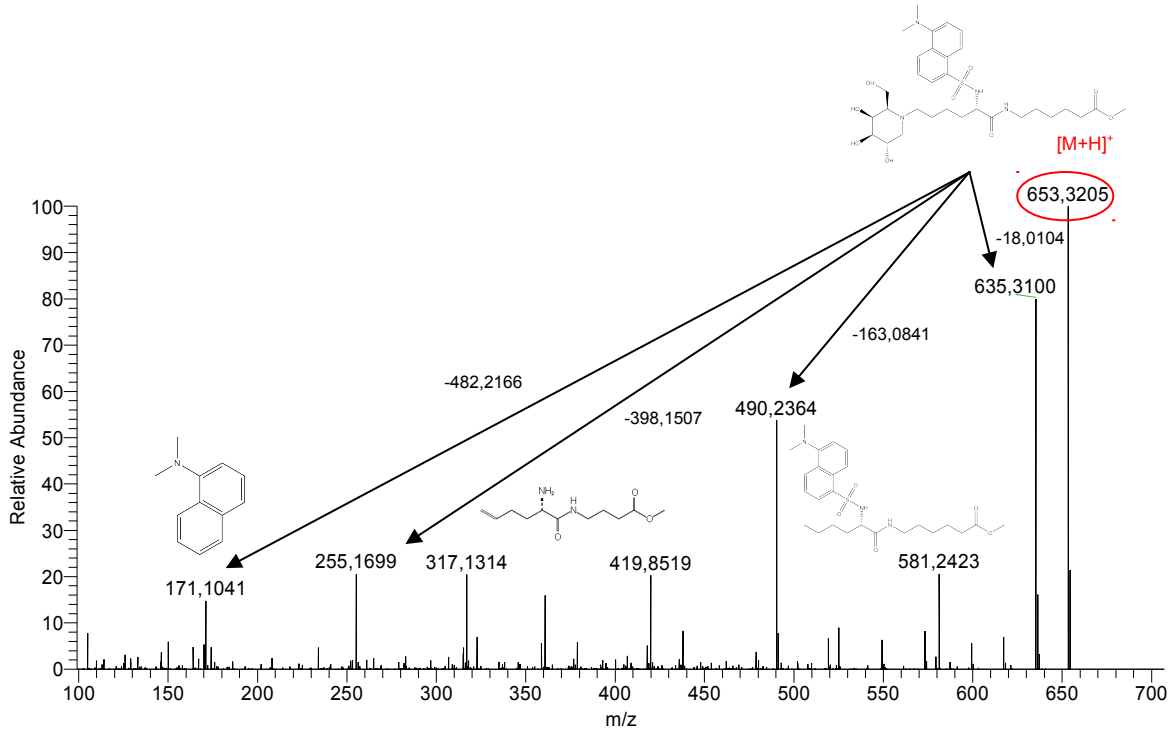

Figure 11: Total ion current of daughter ions from fragmentation of DLHex-DGJ in positive ion mode with a collision energy of 30; Structures of distinct fragments have been annotated where characterization was possible; Marked in red is the parent ion as hydrogen-adduct; Q-Exactive Orbitrap resolution was set to 70.000

Negative ion mode led to the fragmentation pattern which can be seen in figure 12.

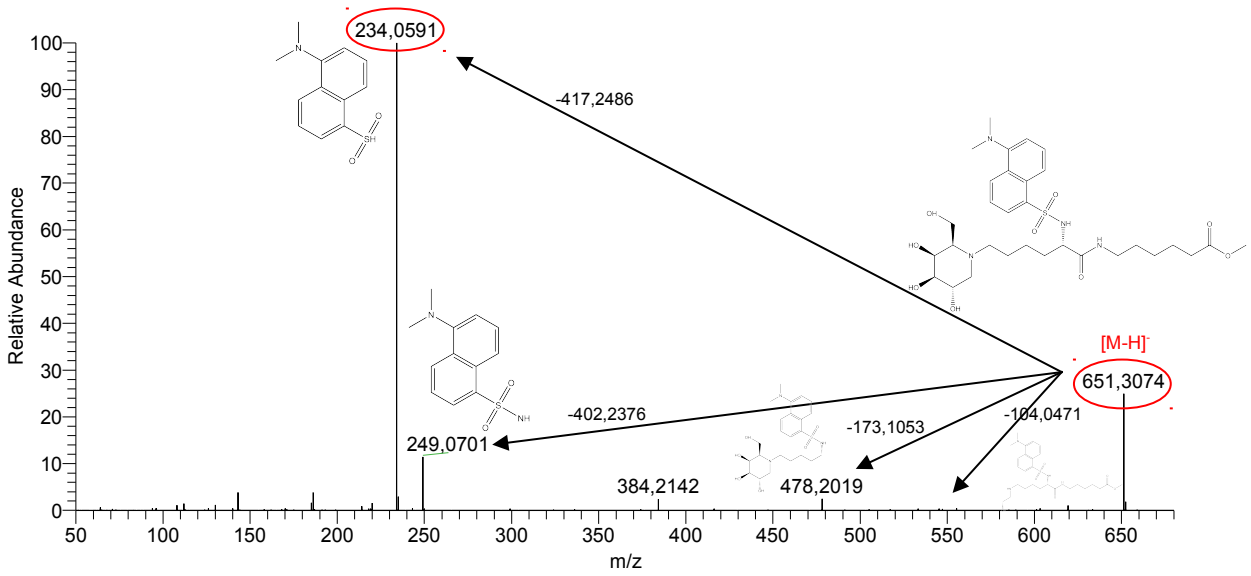

Figure 12: Total ion current of daughter ions from fragmentation of DLHex-DGJ in negative ion mode with a collision energy of 36; Structures of distinct fragments have been annotated where characterization was possible. Marked in red is the parent ion with removal of a hydrogen nucleus; Q-Exactive Orbitrap resolution was set to 70.000

The fragmentation pattern in positive ion mode lead to a vast number of fragments with equally high abundance. It was not possible to annotate a distinct fragment of the parent ion to each peak. In negative mode however, two different forms of the dansyl-group (m/z 234,059 and m/z 249,070) accounted for the better part of the fragments. Two more fragments with low abundance could have been further identified.

Those dansyl fragments, found in high abundance, can desirably be used for further verification of the molecular character of the chaperone. It therefore was decided to do all further measurements in negative ion mode.

Finally, the collision energy could be optimized to yield a maximal amount of the daughter-ion at m/z 234,059. The measured intensities can be seen in figure 13.

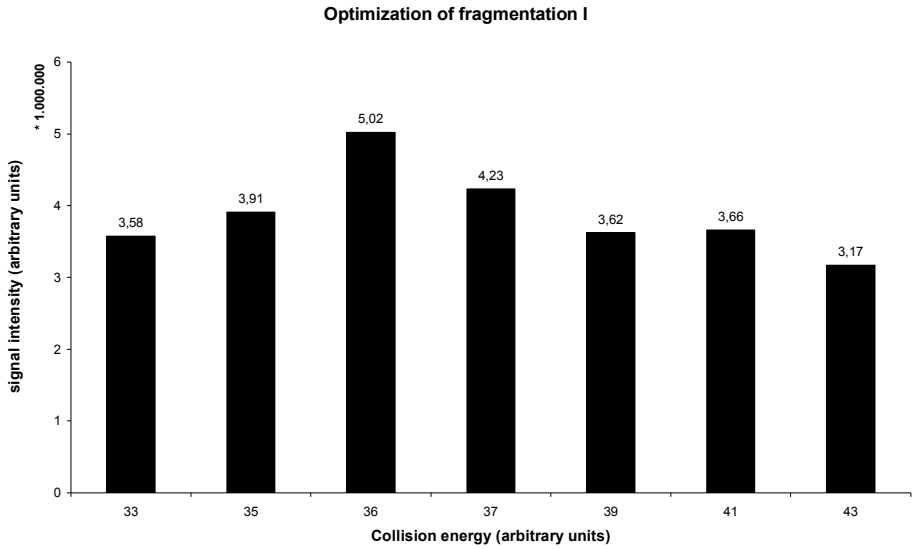

As the experiment was also carried out in the HPLC-MS setup, a further depiction of the effects of altered collision energy on the ion yield in terms of peak area can be seen in figure 14.

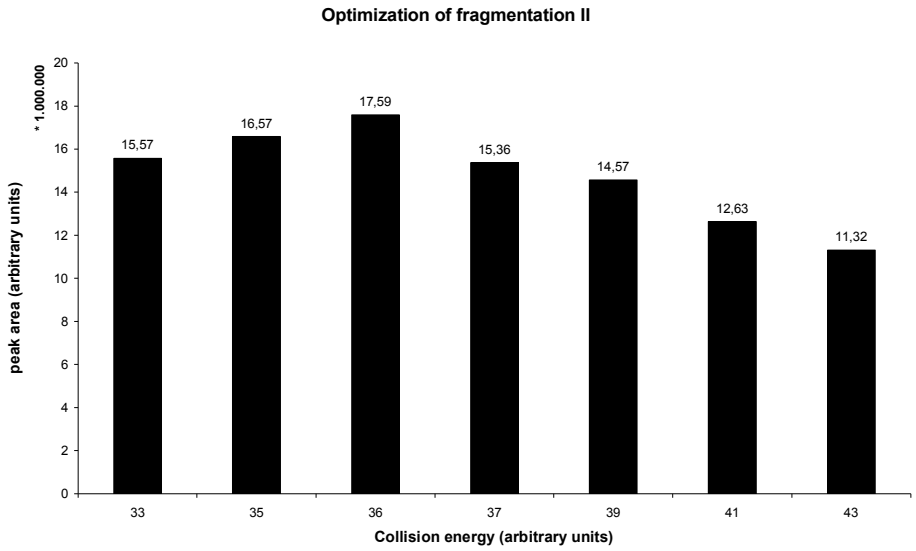

Figure 14: llustration of the effect of different collision energy settings on the yield of daughter-ions with m/z = 234,059 (=dansyl-fragment) ; HPLC setup

As can be derived from the charts in figure 13 and 14, collision energy of 36 units (meaning 36% of the maximal possible collision energy) leads to the highest amount of specific daughter-ions and was therefore used in all further fragmentation experiments.

5.1.3 Optimization of liquid chromatography

To separate the chaperone from any remaining cellular substances after performing the extraction from human skin fibroblasts in the final experiment, it was necessary to perform a kind of chromatographic separation before the sample enters the mass spectrometer. For this case, separation by reversed-phase HPLC was carried out. Initial tests to find the best settings of the ESI probe and the mass spectrometer itself for the higher flow rates were done by injecting dilutions of the chaperone via the HPLC- auto sampler to a tube in order to by-pass the columns and therefore speed up runtimes to do the optimizations more quickly.

The parameters of the ESI probe were modified in the same manner as stated in chapter 4.12.2, varying each element with the objective of maximizing the yield of target ion signal and peak area respectively. At first, his was done for a flow rate of 200 µl/min as well as a flow rate of 300 µl/min. The final settings of the ESI probe can be seen in table 16.

Table 16: Optimization of H-ESI settings for flow rate of 300 µl/min and concentrations of the chaperone of 500 ng/ml in MeOH with formic acid as modifier

Sheath gas pressure (psi)	35
Auxilliary gas flow (arbitrary units)	18
Sweep gas flow (arbitrary units)	0
Ion transfer tube temperature (°C)	330
H-ESI vaporizer temperature (°C)	375
Spray voltage (V)	-5000

To optimize the chromatographic process in presence of the matrix, confluently grown, untreated fibroblasts from 75 cm² flasks were harvested and DLHex-DGJ was added to the pellet in known concentrations, ranging from 50 ng to 1 µg. A crude lipid extraction was carried out and the resulting organic phase was diluted and applied to the HPLC-MS system. Cell harvesting was carried out according to the protocols given in chapter 4.5.3, while lipid extraction was done according to the protocol of Bligh & Dyer.

With the relatively non-polar character of the chaperone in mind, a reversed-phase C18 column (Hypersil Gold 50 x 2,1mm, 3 µm bead size) was used for this experiment.

In order to determine the best fitting mobile phase in terms of elution time of the chaperone, different compositions of methanol and water – each with the addition of formic acid and ammonium acetate as modifiers – were tested. An initial composition of 50% water / 50 % methanol was found best fitting for reasonable chaperone retention. Consequent flushing of the column was achieved by increasing the amount of methanol in order to elute more non-polar substances. The optimized protocol can be found in chapter 4.12.4 in Material and Methods.

Figure 15 shows a chromatogram of both the TIC as well as the XIC for DLHex-DGJ of an optimized run.

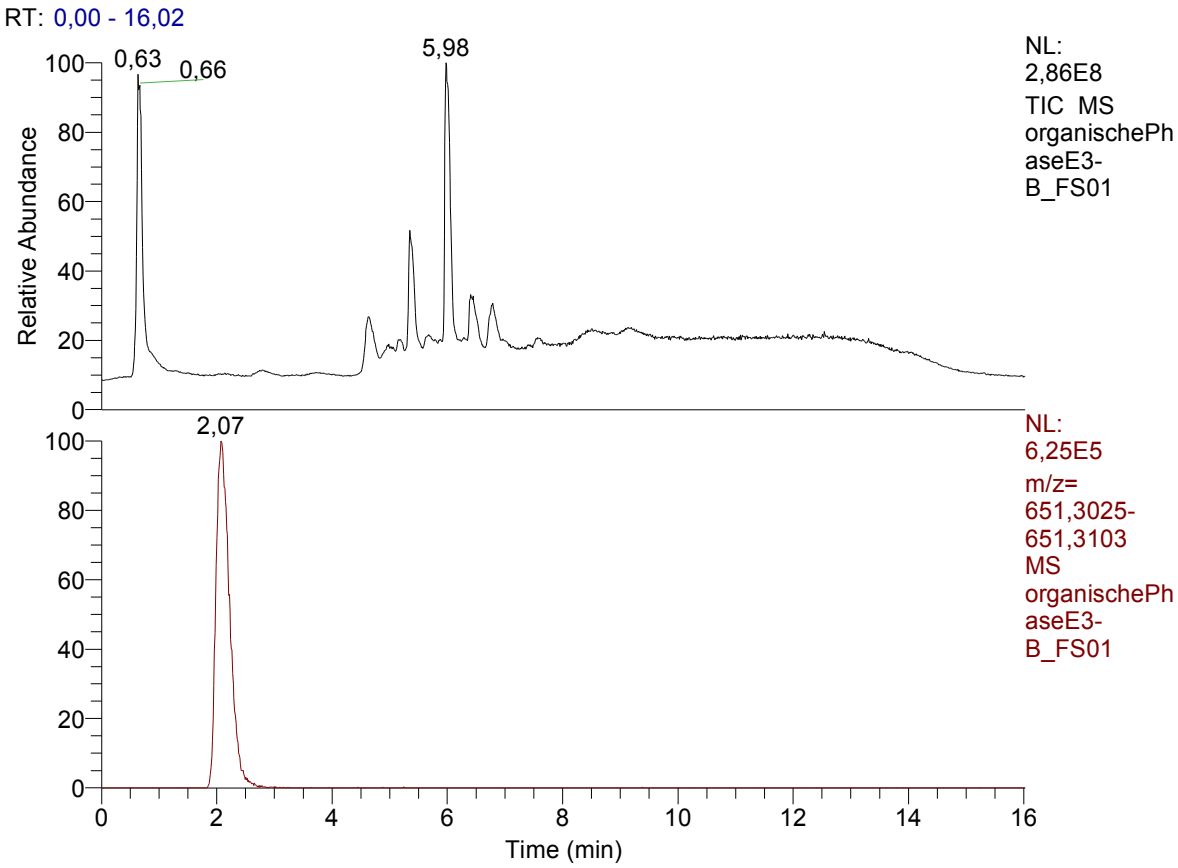

To further confirm the character of the chaperone as well as to increase the yield of target ions, a tandem-MS setup was created, were the fragmentation settings determined in chapter 4.12.3 could have been applied.

Since DLHex-DGJ elutes at roughly 2 minutes, the post-column valve was set to switch from the ESI-source to waste at minute 3 of the run. Thus, unnecessary soiling of the MS

machinery could be avoided without loss of significance and information. No further changes of the HPLC setup were necessary. Figure 16 shows the tandem-MS chromatograms of the same samples as used above.

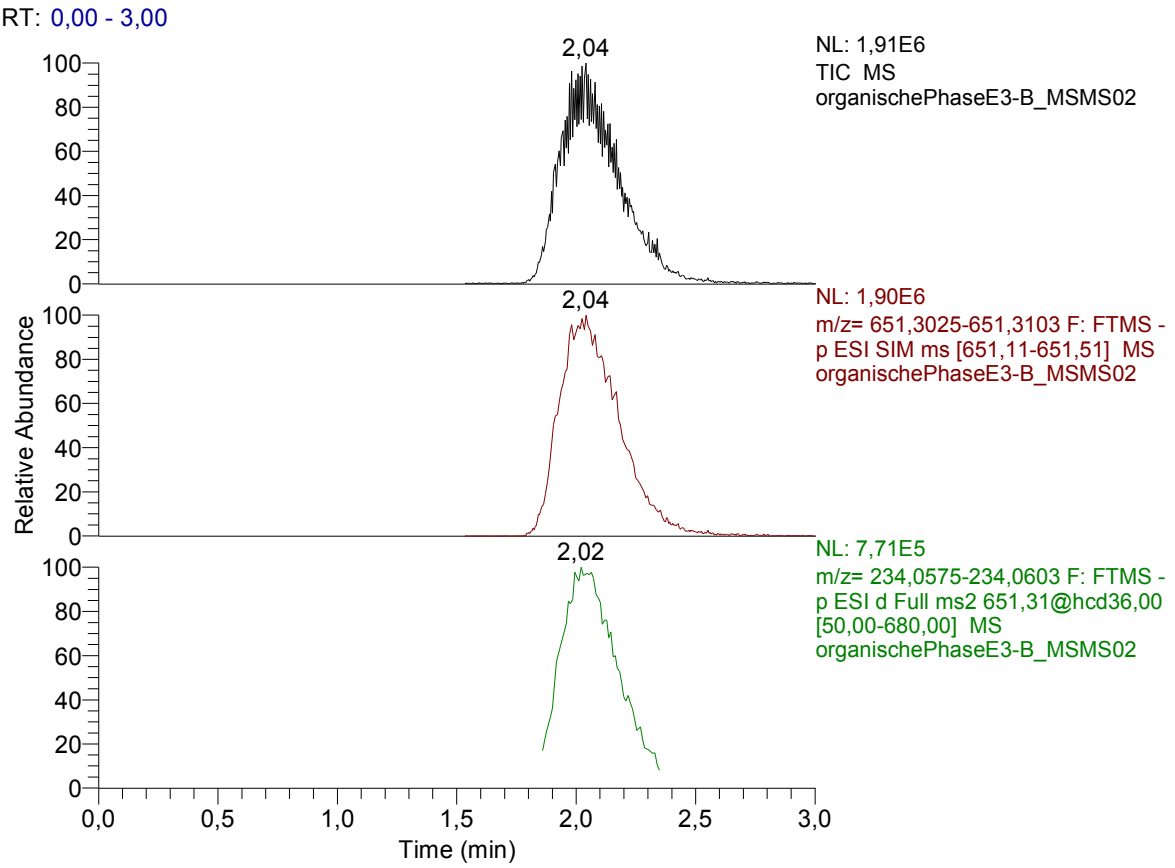

Figure 16: Chromatograms of a 20-fold dilution of the organic phase of a lipid extraction spiked with 1 µg of DLHex-DGJ done with tandem-MS setup; 'TIC' can be seen above, comprising measurements at 651,3 +/- 0,4 m/z as well as fragmentation scans from 50 to 680 m/z. The XIC for the chaperone with an m/z of 651,3067 +/- 6 ppm ([M-H]-) can be seen in the middle. Bottommost is an XIC for the dansyl-fragment of the chaperone where the m/z range is set at 234,0590 +/- 6 ppm

As final optimization step of the MS settings, dynamic exclusion was set to 20 seconds. This affects the frequency of fragmentation steps carried out by the instrument. As the area of the molecule-peak is used for concentration determination and the dansyl-fragment just serves as secondary conformation, it was considered adequate to sacrifice the yield for the dansyl-fragment – at least up to a certain degree – in order to improve scan-rate and therefore peak-shape of the molecule-ion.

To conclude, the character of the substance could be determined in three different ways.

Firstly by comparison of HPLC retention times, secondly by high accuracy molecular weight determination of the parent ion at 651,3067 +/- 6 ppm for $[M-H]^-$ in negative ion mode and thirdly by high accuracy molecular weight determination of the dansyl-fragment at 234,0590 +/- 6 ppm for $[M-H]^-$.

5.1.4 Lipid extraction

To separate the chaperone from cellular debris and efficiently recover the molecule from harvested fibroblasts, an efficient extraction protocol had to be set up. For a first approach, an existing Bligh and Dyer – protocol was employed. Hence, a fibroblast pellet, harvested from a confluently grown 75 cm² culture flask, was spiked with a total amount of 1 µg DLHex-DGJ. After extraction, both organic and aqueous phase were diluted and measured via the same standard HPLC-MS method. Calculation of the extraction-efficiency was done by the use of a calibration equation (see chapter 4.12.5.1) Roughly half of the amount of chaperone initially added was found in the organic phase, while the recovery in the aqueous phase was less tha 4%. The rest of the material (approx. 45%) obviously was held back in the protein layer.

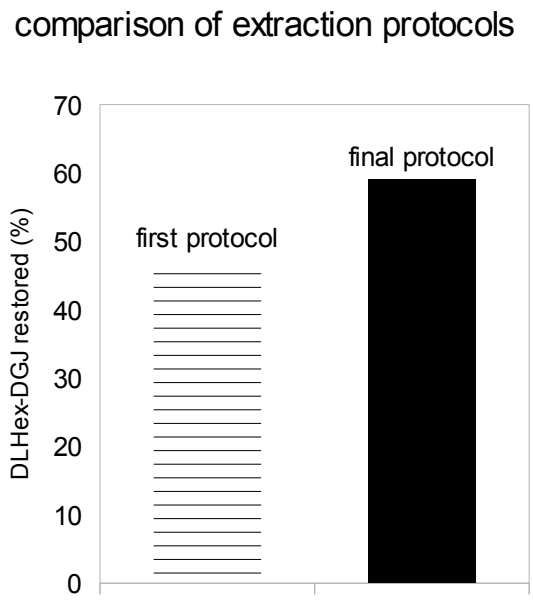

Figure 17: Comparison of the restoration of DLHex-DGJ between the standard lipid extraction protocol and the optimized version; Restoration was calculated by the use of the calibration curve given in chapter 4.12.5.1

Based on these observations, the extraction protocol was modified to increase the yield of target-substance in the organic phase. Two more iterations of the extraction procedure were added and resulting organic phases were pooled and reduced under a stream of nitrogen.

The final protocol resulted in a recovery of roughly 60% of the initially added chaperone, which was considered sufficient for the purpose. Detailed data of the method

development procedure is not shown, however, the difference between initial and final extraction protocol is depicted in figure 17.

5.1.5 Solid phase extraction

As stated in Chapter 4.7, a step of sample clean-up had to be added before routine application of fibroblast lipid extracts to the HPLC system. This also became necessary as the optimized lipid extraction protocol not only resulted in enrichment of the target substance but also in a general concentration of contaminants.

A first attempt was made to achieve this goal via preparative chromatography, using silica gel columns.
For this purpose, preliminary tests were made with thin layer chromatography (TLC) to identify a suitable solvent for the following column chromatography. For identification of DLHex-DGJ on the TLC plate and for calculation of its R_f-value – optimally between 0,5 and 0,8 – the fluorescence of the dansyl group could be identified and labeled under ultraviolet light. A mixture of ethyl acetate and methanol at a ratio of 1:4 was found to generate a Rf-value of 0,53 and was therefore used for the further experiments.

Greiner columns equipped with a frit were manually filled with silica gel (Roth, silica gel 60, < 0,063 mm) and elutriated with an excess of solvent. After addition of an appropriate amount of chaperone, dissolved in ethyl acetate and methanol, elution was done and fractions were collected in glass tubes. In analogy to the previous TLC procedure, ultraviolet light was used to rapidly identify chaperone-rich fractions. However, no fluorescence was detectable throughout the fractions, while most of the signal could be found on the column itself, probably due to the hydrophobic character of the chaperone. Therefore, the normal-phase columns were replaced by Varian© Bond Elut C18 reversed-phased columns.

As first attempts with water as washing solvent and methanol as eluting solvent turned out promising, the method could be further optimized. After sample application, water was used as a washing solvent to elute more polar contaminants. Thereafter, a further washing step with the use of n-hexane was included, which would eliminate more non-polar components.

Final elution of the chaperone was optimized with the application of a methanol-water mixture to efficiently relieve the target substance. Elution efficiency was monitored both by ultraviolet light observation for rapid evaluation as well as by application of the optimized MS protocol for quantitative measurements. In parallel, several full scan measurements were done in order to monitor the quality of the clean-up.

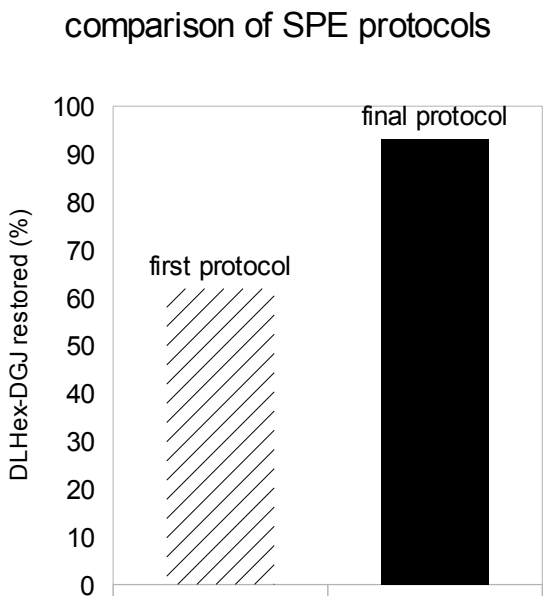

Figure 18: Comparison of the restoration of DLHex-DGJ between the first SPE protocol and the optimized version; Restoration was calculated by the use of the calibration curve given in chapter 4.12.5.1

In the course of numerous optimization steps, an extraction efficiency of over 90 % was achieved, which – in combination with prior lipid extraction – leads to a total extraction efficiency of roughly 55 %. The final protocol can be found in chapter 4.7.

5.1.6 LOQ/LOD/MDL

In order to determine the limitations of the detection instruments as well as of the entire extraction procedure, the limits of quantification and detection were determined.

The ratio of peak height to background noise was calculated for several samples and displayed as a function of concentration. The calibration curve generated to calculate LOD and LOQ can be seen in figure 19.

Limit of detection

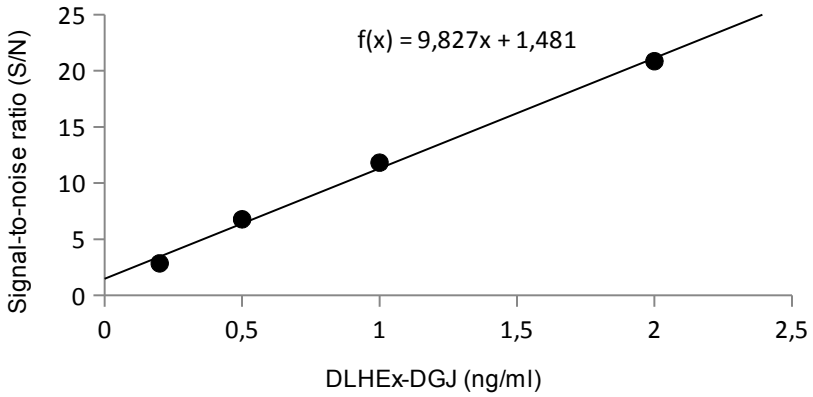

Via transformation of the formula, the limit of detection for pure DLHex-DGJ was calculated to be 155 pg/ml, while the limit of quantification accounts for 765 pg/ml. As the minimal injection volume of the autosampler was set to 10 µl per run, a total number of 1,55 pg as LOD and 7,65 pg as LOQ per sample could be calculated.

The method detection limit was calculated in an analogous way. Graphical display of the calibration curve can be found in figure 20.
As before, transformation of the equation resulted in a calculated MLD of 1,15 ng/ml and an MLQ of 3,59 ng/ml. Enrichment of samples up to a volume of 10 µl consequently leads to an MLD of 11,5 pg and an MLQ of 35,9 pg. For practical reasons, a minimal sample volume of 50 µl was considered applicable in terms of sample handling. Ergo, a MLD of 57,5 pg per sample and a MLQ of 179,5 pg per sample were calculated.

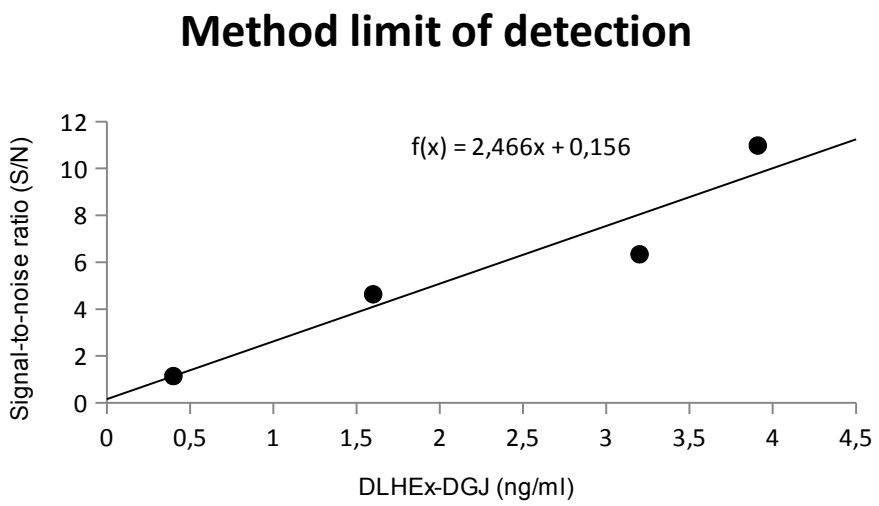

Figure 20: MLD calibration curve; For calculation of the calibration curve, low concentrations of DLHex-DGJ underwent the full extraction protocol and were outlined against their signal-to-noise ratio (S/N)

5.2 Cell-based experiments

Procedures regarding the application of DLHex-DGJ to cultured fibroblasts as well as cell handling and harvesting are described in the Material & Method section, chapter 4.5.

As for quantification procedures, it was considered appropriate to generate a calibration curve were calibratory samples underwent the same extraction and cleaning procedures as the samples in order to compensate for the absence of an internal standard.

Cell-based experiments were carried out based primarily on the findings of Fantur et al. [21]. Therefore, if not stated differently, 6-well plates were used to grow fibroblasts for uptake experiments.

Data on the amount of chaperone is given as ng per sample. If not stated differently, cells were harvested at confluency. Because of the differing extraction procedures of chaperone- and protein-determination protocols, it was not possible to determine both attributes from the same sample. Therefore mean values of protein concentrations of confluently grown fibroblasts in 6-well plates were determined and chaperone concentration was referred to calculated mean protein concentrations.

5.2.1 Validation of harvesting procedure

In order to validate the harvesting procedure and ensure adequate recovery of the chaperone, several control experiments were done beforehand.

Firstly, concentration of the chaperone in the culture medium as well as the supernatant from cleaning steps prior to the cell harvest were measured. This was done as evaluation of the accuracy of the calibration curve, as the calculated amount of DLHex-DGJ shall match the applied amount in the supernatant as well.
Triplicate measurement showed an average recovery of 90% of DLHex-DGJ in the culture medium.

Secondly, background noise of the chaperone was evaluated by application of the standard extraction protocol to wells that were free of cells, but were otherwise treated the same way as sample-wells. The background noise of DLHex-DGJ for different concentrations in culture medium can be found in table 17.

Table 17: Measurement of background noise of DLHex-DGJ at different concentrations in culture medium; Concentrations found are based on triplicate measurements

Background noise		
Concentration in medium (µM)	Amount of DLHex-DGJ per well (µg)	Background (ng/sample)
20	39,17	0,086
40	78,33	0,103
50	97,92	0,227
100	195,84	0,721
250	489,6	0,801
500	979,2	4,352

Subsequently, this background noise was subtracted from every sample where this was applicable in terms of chaperone concentration and growing conditions.

5.2.2 Uptake of DLHex-DGJ in dependence of concentration

As data of Fantur et al. [21] showed a saturation effect of higher concentrations of DLHex-

DGJ on the restoration of β-galactosidase activity, concentrations for uptake experiments were chosen accordingly. In further accordance with the work of Fantur et al., incubation time of the cells was 96 hours.

In a first experiment, this was done with human skin fibroblasts obtained from a healthy patient. The result can be seen in figure 21. For every data point, at least five biological replicates were made in order to compensate for the loss of accuracy in sample preparation.

In contrast to the saturation effect for ß-gal activity, observed by Fantur et al., the amount of DLHex-DGJ restored from cultured fibroblasts increased linearly with the concentration offered via the culture medium. Increase of DLHex-DGJ concentration beyond 500 µM in the culture medium led to death of the cultured fibroblasts.

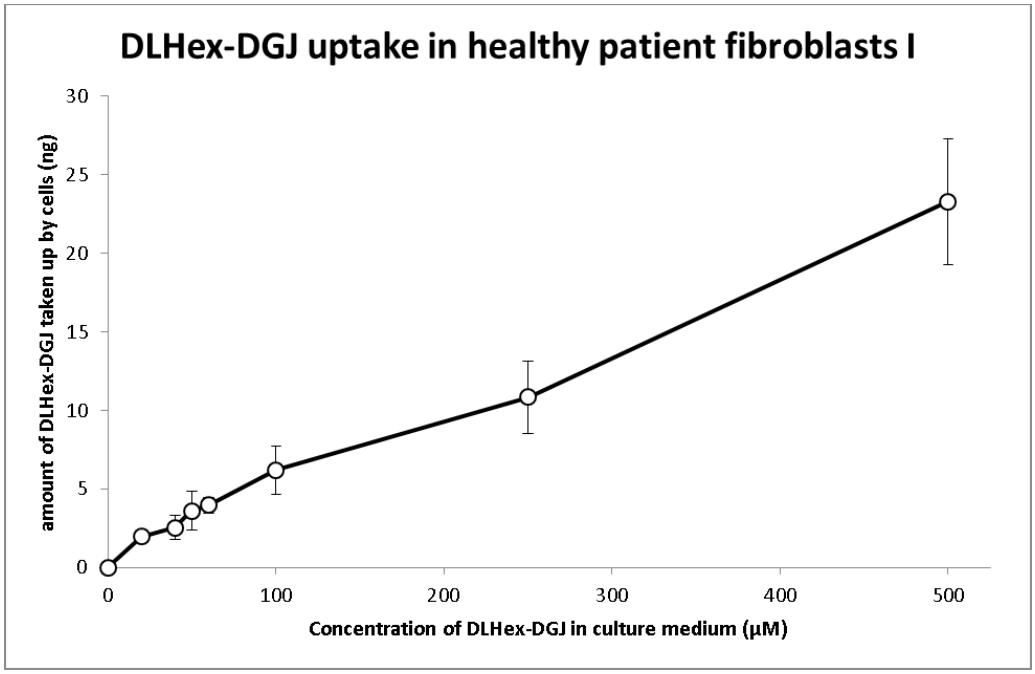

Figure 21: Uptake of DLHex-DGJ in wildtype fibroblasts; harvesting and extraction were performed according to protocols; background already subtracted

As all cells in this assay were grown to confluency, it was assumed that the total amount of cell protein per well should be approximately equal. Therefore the protein content of more than 40 wells was averaged to a number of 131 µg per well (SD +/- 32,0 µg) and used as mean cell protein value for the following experiments, if not stated differently.

The same measurements were done with the use of a mutant cell line, previously proven to be chaperone-sensitive ([13], [21]) with the missense mutation comprising p.R201C in exon 6 of the *GLB1* gene coding for β-galactosidase. Figure 22 shows the total uptake of DLHex-DGJ, the uptake relative to the cell protein content is not shown.

Equally to the healthy patient cells, no saturation effect was found on the uptake of DLHex-DGJ. Apart from a slightly inconsistent peak at a DLHex-DGJ concentration of 100 µM in the culture medium, the amount of intracellular fibroblast chaperone increased linearly with the chaperone concentration in culture medium.

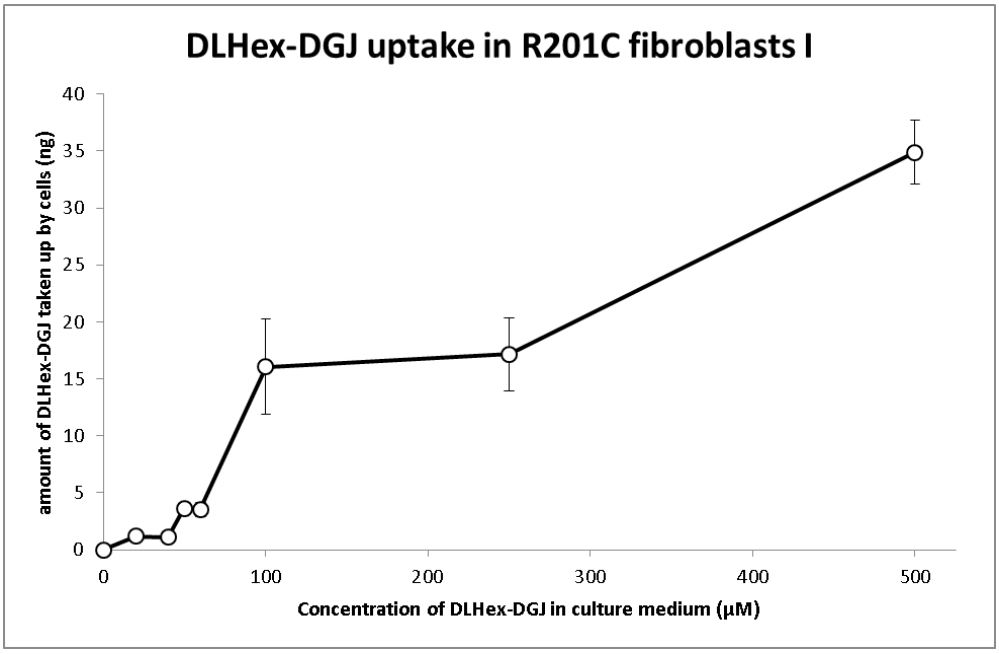

Figure 22: Uptake of DLHex-DGJ in fibroblasts carrying the p.R201C mutation in GLB1; harvesting and extraction were performed according to protocols; background already subtracted

Figure 23 finally shows the direct comparison of healthy and mutant fibroblast cell line in terms of chaperone uptake. Interestingly, the amount of chaperone isolated at lower concentrations was lower in p.R201C cells than in healthy patient cells. At the three topmost concentrations however, p.R201C cells seem to have taken up significantly more chaperone from the medium than healthy patient cells (p-value < 0,01 for 100 and 250 µM and < 0,05 for 500 µM).

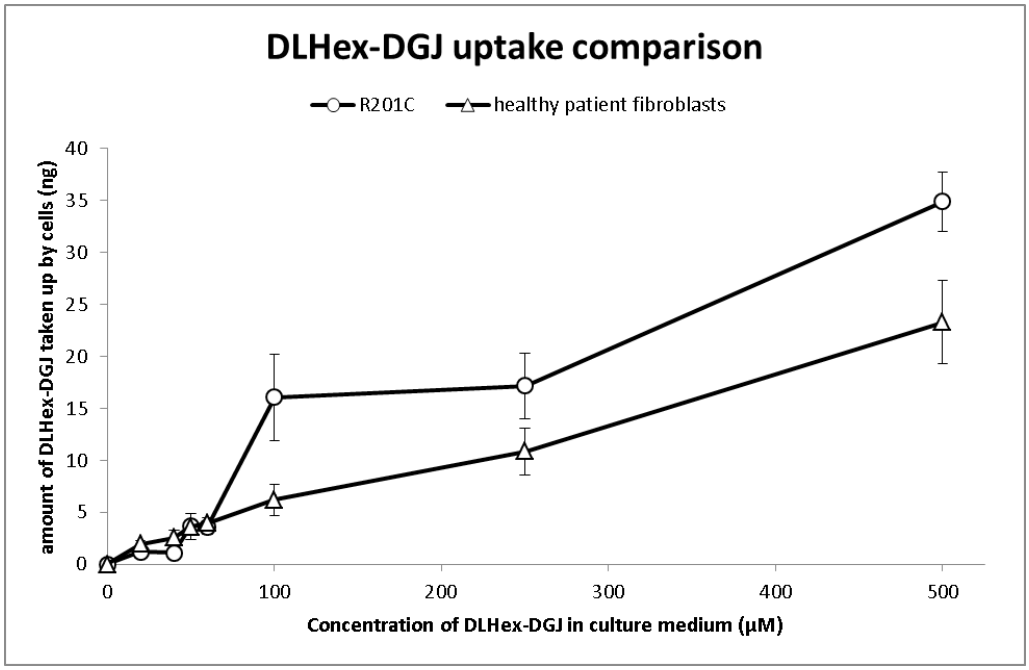

Figure 23: Comparison of the uptake of DLHex-DGJ in wildtype fibroblasts and fibroblasts comprising the p.R201C mutation in GLB1

5.2.3 Time course of DLHex-DGJ uptake in dependence of time

To further investigate on the uptake kinetics of DLHex-DGJ, cells were harvested after different durations of exposure to 20µM chaperone. This concentration was chosen because it was shown in experiments of Fantur et al. ([21]) that 20 µM of DLHex-DGJ is the lowest concentration sufficient to restore the enzymatic activity to more than 10 % of the wildtype level. The importance of this value is explained in chapter 2.1.5.
Different timepoints were specified at which the cells were harvested after chaperone treatment. In a first approach, this was done for a time-frame between 24 to 96 hours after DLHex-DGJ exposure. Healthy patient cells were used. The resulting uptake curve can be found in figure 24. The detected amount of DLHex-DGJ at the 12 hour time point is approximately the same as after 96 hours of incubation. The measured amount of chaperone taken up by the cells shows a slight increase over the period from 12 to 72 hours and decreases again at 96 hours incubation time.

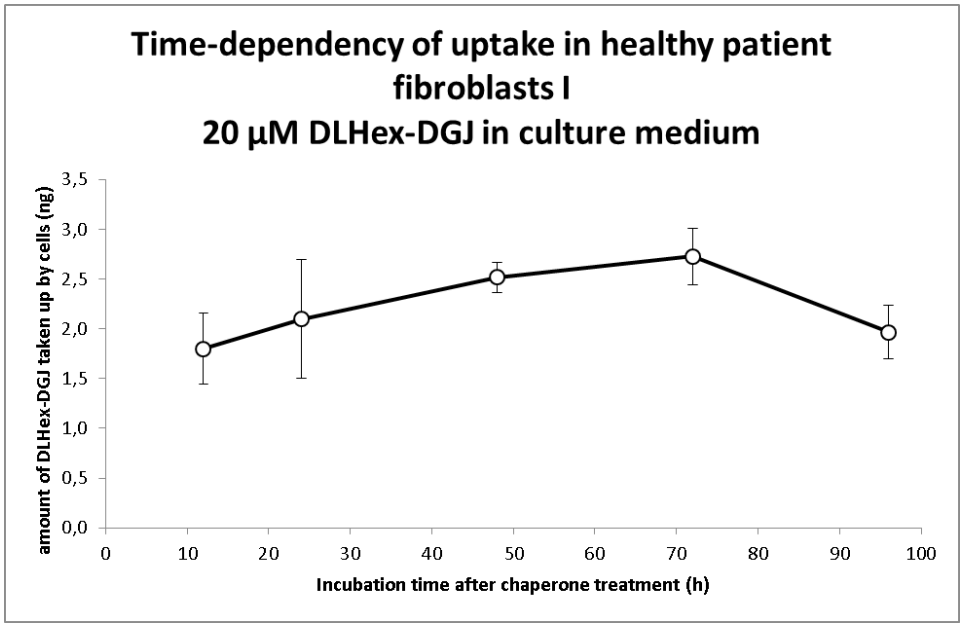

Figure 24: Uptake of DLHex-DGJ in wildtype fibroblasts after different incubation times; Chaperone concentration was 20 µM in culture medium; background already subtracted

As in this case cells were harvested at considerably differing time points, control cells were grown in parallel and used for protein determination. Calculated amount of DLHex-DGJ per cell protein after different incubation times can be seen in figure 25.

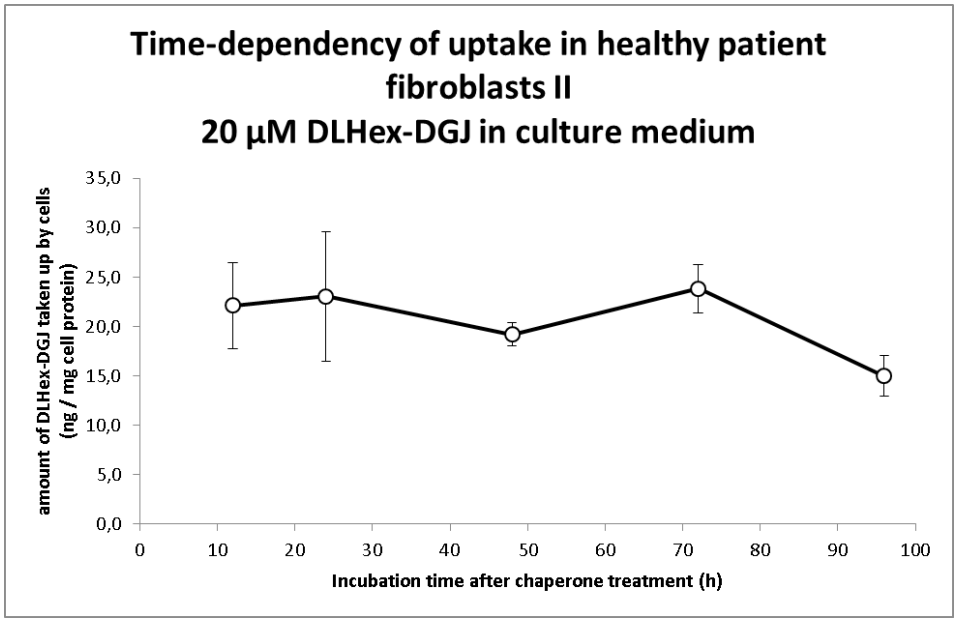

Figure 25: Uptake of DLHex-DGJ in wildtype fibroblasts after different incubation times relative to cellular portein level; Chaperone concentration was 20 µM in culture medium; background already subtracted

With reference to the estimated protein content of the cells, the increase of DLHex-DGJ uptake can be balanced, as there is no significant change in chaperone concentration per cell protein between 12 and 72 hours of incubation time. The slight decrement at 96 hours of incubation time remains, but the value not significantly lower than at the other time-points (p-value > 0,1).

As the evaluation of these first time-dependent assays showed a saturation effect of the uptake of DLHex-DGJ already at the first time-point at 12 hours, a successional assay was planned with time-points set between two and 24 hours.

This assay was carried out three times independently, with three biological replicates at each time-point respectively. Cell-line in use was mutant line p.R201C. As 3 wells of a 6-well plate were used for chaperone determination, the remaining 3 wells were available to measure β-galactosidase activity and protein concentration at each time-point.

A graphical representation of the chaperone-uptake can be found in figure 26, while β-galactosidase activities are to be found in chapter 5.2.4.

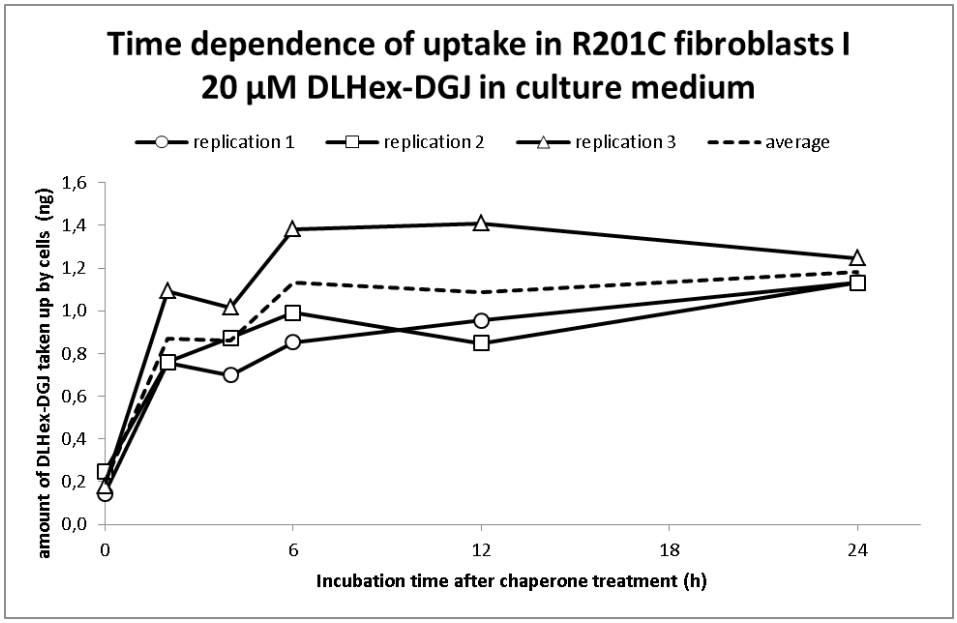

Figure 26: Uptake of DLHex-DGJ in fibroblasts comprising the p.R201C mutation in GLB1 after different incubation times; Chaperone concentration was 20 µM in culture medium; Experiment was carried out as triplicate with three replications respectively; background already subtracted

The dotted line in figure 26 shows the averaged values of the three replications. For the 0

hours time-point, cells were incubated with the chaperone for roughly five minutes before the washing procedure described in chapter 4.5.3 was applicated. The amount of DLHex-DGJ detected after two and four hours of incubation is significantly lower than at 6 hours of incubation (p-values < 0,05), at which time the concentration of DLHex-DGJ seems to reach its final level. Figure 27 shows the same data with respect to the cellular protein level.

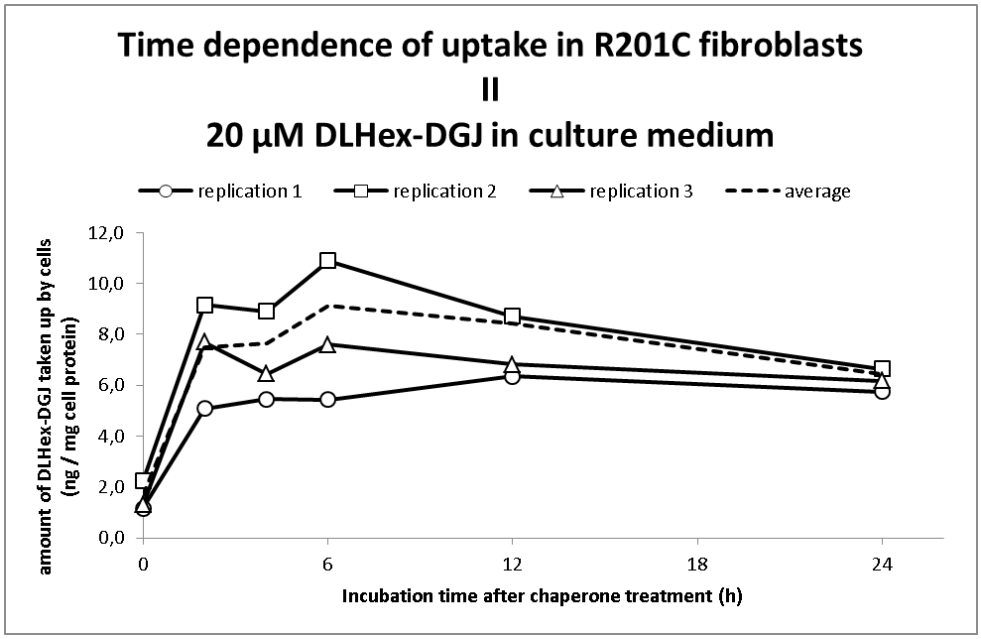

Figure 27: Uptake of DLHex-DGJ in fibroblasts comprising the p.R201C mutation in GLB1 after different incubation times relative to cellular portein level; Chaperone concentration was 20 µM in culture medium; Experiment was carried out as triplicate with three replications respectively; background already subtracted

In a further experiment the release of DLHex-DGJ from fibroblasts was monitored. Cells were treated with 20 µM DLHex-DGJ for 12 hours. At this point, chaperone-rich medium was removed and cells were washed two times with sterile 0,9 % NaCl. Fresh, chaperone-free medium was added, cells were harvested at given time-points and remaining DLHex-DGJ content in cells was measured as well as β-galactosidase activity and protein content.

Figure 28 shows the average amount of DLHex-DGJ found in fibroblasts at given time points but with addition of the release-curve.

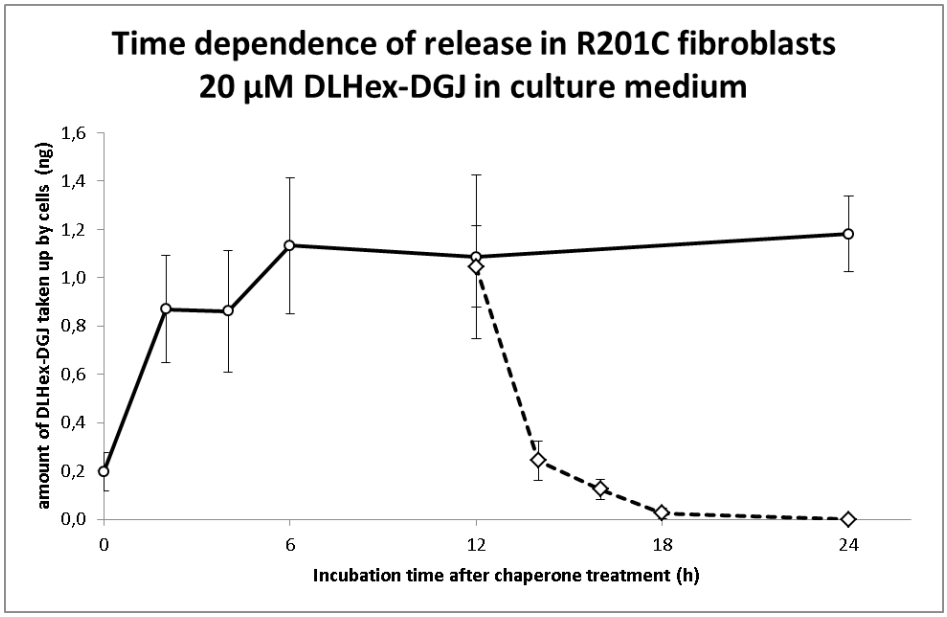

Figure 28: Uptake of DLHex-DGJ in fibroblasts comprising the p.R201C mutation in GLB1 after different incubation times; Chaperone concentration was 20 µM in culture medium; After 12h of incubation, culture medium was replaced with chaperone-free medium, indicated by the dotted line; background already subtracted

Two hours after removal of the chaperone-rich medium, the detected concentration of DLHex-DGJ reached a level similar to the 0 hour time point, where the cells were incubated in chaperone-rich medium for 5 minutes. After four more hours, the concentration of DLHex-DGJ was found to be below the limit of detection.

Therefore, uptake and release of the chaperone to the cultured cells seem to follow the same kinetics.

5.2.4 Effects of chaperone treatment on β-galactosidase activity

Influence of the concentration of the chaperone DLHex-DGJ on the in vitro activity of β-galactosidase have been studied before by Katrin Fantur et al [21]. However, no time-related studies on the change of β-galactosidase activity were made. In order to correlate the uptake experiments described in the chapter before with the relative activation of β-galactosidase in vitro, the following enzyme assays were carried out.

In correspondence with the experiment described in chapter 5.2.3, β-galactosidase

activity was measured in three replications over a time-course of 24 hours after treatment with DLHex-DGJ. The result can be seen in figure 29.

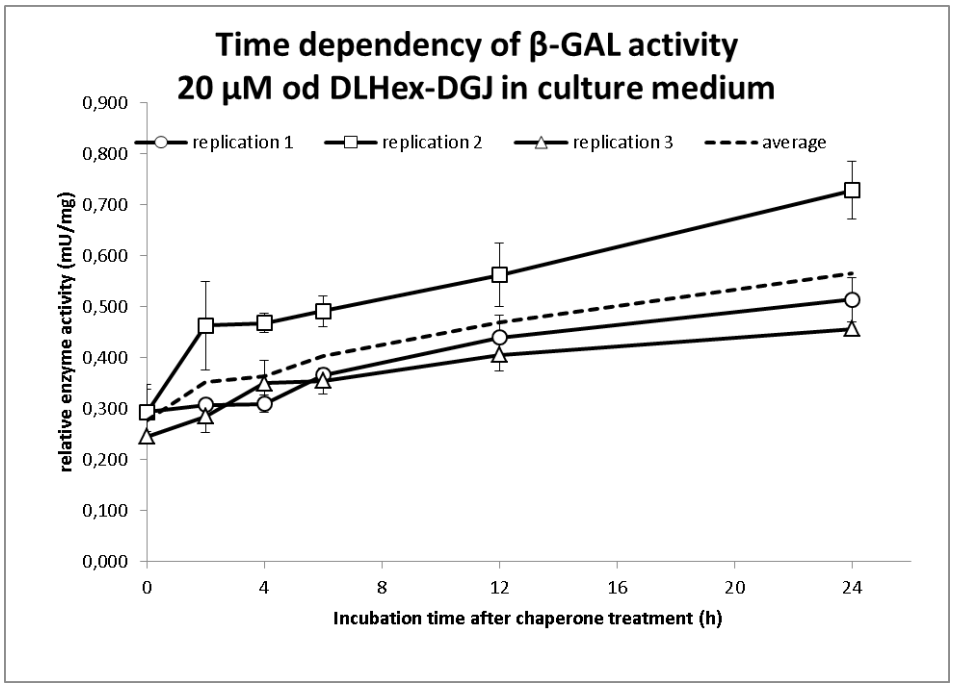

Figure 29: Relative enzymatic activity of β-galactosidase in p.R201C fibroblasts after incubation with 20 µM of DLHex-DGJ at varying durations; Experiment was carried out as triplicate with three replications respectively

Dissimilar to the uptake of DLHex-DGJ, the restoration of β-gal activity increases linearly over the selected time frame.

In an analogue way, the release of DLHex-DGJ, as described in chapter 5.2.3, was monitored as loss of activity of β-gal in vitro. The corresponding graph, alongside with a comparison to the uptake and release of chaperone relative to the protein content, can be seen in figure 30.

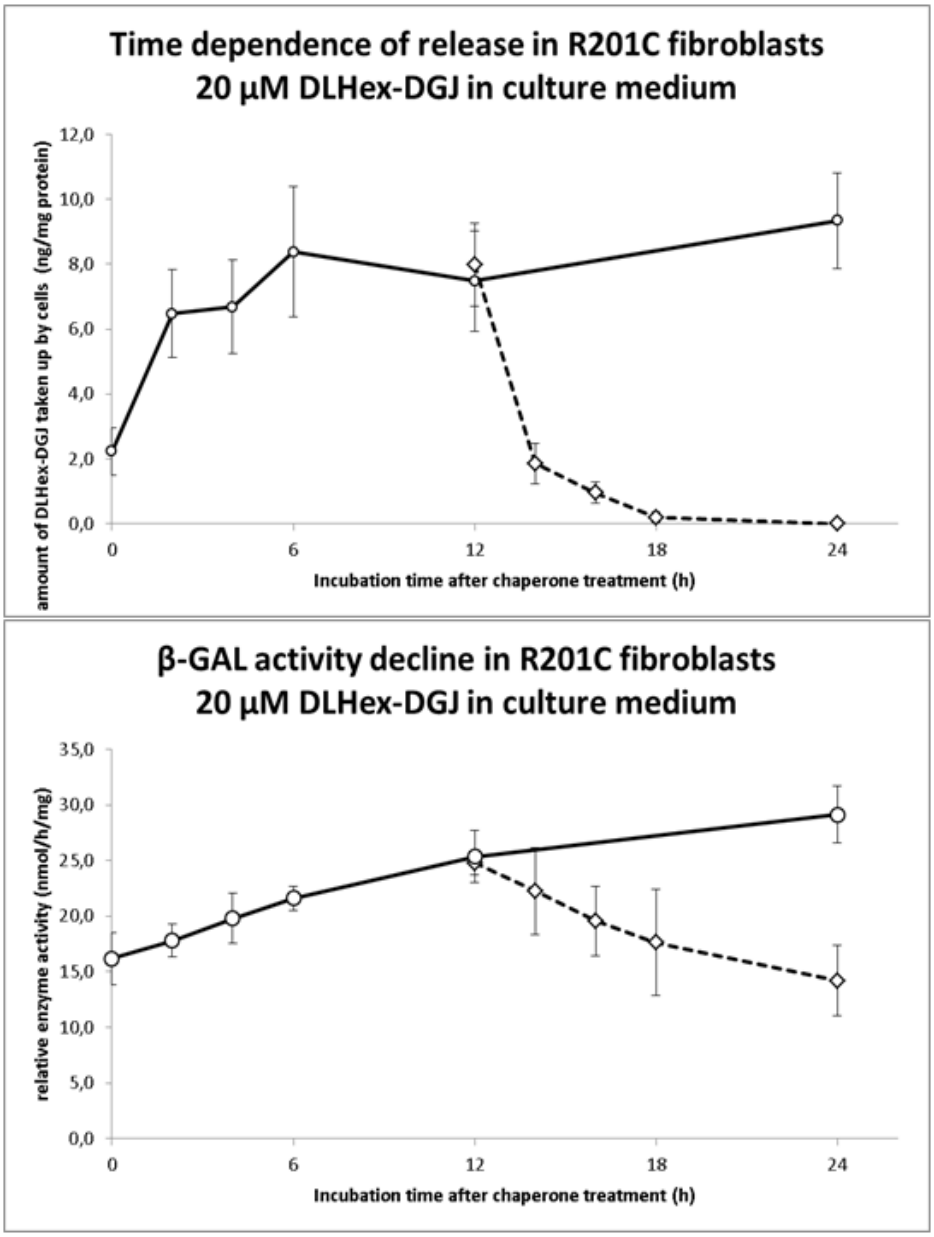

Figure 30: ***Comparison of time courses of uptake and release of DLHex-DGJ and resulting ß-gal activity.*** *(B) shows the relative enzymatic activity of ß-galactosidase in p.R201C fibroblasts after incubation with 20 µM of DLHex-DGJ at varying durations; After 12h of incubation, culture medium was replaced with chaperone-free medium, indicated by the dotted line; (A) shows the intracellular content of DLHex-DGJ for the purpose of comparison.*

Once again, the effects on β-gal activation seem to follow a more linear kinetic than the uptake of the chaperone itself. While the intracellular concentration of DLHex-DGJ reaches its final level after 6 hours, the activity of β-gal continues to increase for at least 24 hours.

After removal of DLHex-DGJ from the medium, the activity of β-gal starts to decline again and no plateau-effect can be seen. 12 hours after the removal of chaperone-rich medium, β-gal activity reaches the same level as in untreated p.R201C fibroblasts.

5.2.5 Effects of chaperone treatment on β-galactosidase maturation

In a similar approach, the effects on chaperone maturation were monitored via a Western Blot. This was done to characterize the uptake dynamics of the pharmacological chaperone and its time dependent effects on protein processing.

For this purpose, p.R201C fibroblasts were cultured in 75 cm² flasks. Cells were treated with 20 µM DLHex-DGJ and harvested at given time points. After protein content determination, samples were diluted to a concentration of 30 µg/ml and after addition of loading buffer and reducing agent, 15 µl per sample were loaded to SDS gels. All further processing was done according to the protocol given in chapter 4.8.

After 45 minutes of alkaline phosphatase reaction, the membrane was dried and scanned. As can be seen, the amount of mature β-gal protein at around 64 kDa does not change significantly between untreated fibroblasts and fibroblasts harvested after two and four hours of chaperone treatment. However, longer incubation times of six, twelve and 24 hours led to an increasing amount of mature β-gal protein, albeit at much lower concentrations than in healthy fibroblast cells. In an analogue fashion, the amount of β-gal precursor protein, visible at around 84 kDa, shows a similar decrease in dependence of incubation time with the chaperone.

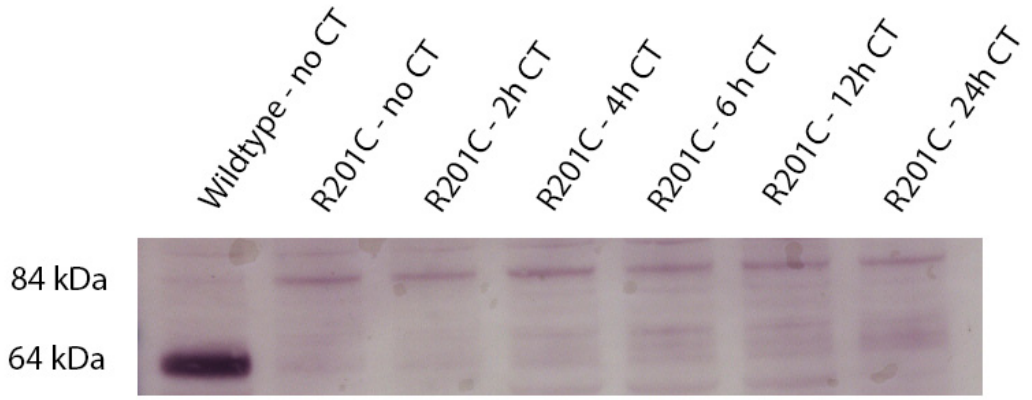

Figure 31: Western Blot with Anti-β-GAL antibody; The mature enzyme can be seen at 64 kDa while the unmatured form has a molecular weight of around 84 kDa; Untreated (no CT) wildtype on lane 1 is compared to untreated p.R201C mutant on lane 2 and p.R201C mutants treated with DLHex-DGJ (CT) over different time-courses in lanes 3 to 7

5.2.6 Digitonin treatment

Treatment of cells with digitonin leads to a permeabilization of the cell membrane. At low concentrations, digitonin primarily interacts with the cytoplasmic membrane and leads to release of cytosolic components, leaving cellular organelles intact. Upon further increase of digitonin concentration, lysosomes become leaky and release their content of small molecules as well as lysosomal enzymes.

For this experiment, p.R201C cells were grown in 25 cm² flasks and treated with 20 µM of DLHex-DGJ for 72 hours. After trypsinization, cells were treated according to the protocol listed in chapter 4.11 with five different concentrations of digitonin diluted in 0,25M sucrose buffer. 150 µl of each fraction was used for chaperone determination, while the remaining 250 µl were ultrasonicated and used to determine the enzymatic activities of β-hexosaminidase and lactate dehydrogenase respectively.

Tables 18 and 19 show the data on the enzymatic activities, while the amount of chaperone found in the fractions can be seen in table 20. A graphical representation thereof can be found in figure 32.

Table 18: LDH activity measurement after treatment of p.R201C mutants with increasing concentrations of digitonin; Digitonin concentration as well as enzymatic activity are indicated relative to the cellular protein content measured photometrically

Digitonin treatment – LDH activity				
µg/mg digitonin	Fraction	Activity (mU/mg)	% soluble	% recovery
0	whole lysate	1435,9	9,0	89,7
	pellet	1171,5		
	supernatant	116,5		
2,06	whole lysate	1721,0	8,5	97,9
	pellet	1541,3		
	supernatant	144,0		
5,05	whole lysate	1188,2	4,5	105,5
	pellet	1197,3		
	supernatant	56,4		
18,12	whole lysate	1461,96	41,9	89,6
	pellet	760,9		
	supernatant	548,9		
41,6	whole lysate	1316,1	93,0	99,2
	pellet	91,5		
	supernatant	1213,8		

Table 19: β-HEX activity measurement after treatment of p.R201C mutants with increasing concentrations of digitonin; Digitonin concentration as well as enzymatic activity are indicated relative to the cellular protein content measured photometrically

Digitonin treatment – β-Hexosaminidase activity				
µg/mg digitonin	Fraction	Activity (mU/mg)	% soluble	% recovery
0	whole lysate	11,158	1,8	92,1
	pellet	10,093		
	supernatant	0,183		

Digitonin treatment – β-Hexosaminidase activity				
2,06	whole lysate	17,871	3,0	86,7
	pellet	15,021		
	supernatant	0,466		
5,05	whole lysate	11,967	2,1	87,7
	pellet	10,278		
	supernatant	0,216		
18,12	whole lysate	14,401	3,1	71,7
	pellet	10,006		
	supernatant	0,325		
41,6	whole lysate	16,815	10,0	83,0
	pellet	12,564		
	supernatant	1,391		

Table 20: Measurement of DLHex-DGJ content after treatment of p.R201C mutants with increasing concentrations of digitonin; Digitonin concentration is indicated relative to the cellular protein content measured photometrically; Chaperone-concentration is given as total amount of DLHex-DGJ measured per fraction

Digitonin treatment – DLHex-DGJ detection				
µg/mg digitonin	Fraction	ng / fraction	% soluble	% recovery
0	whole lysate	1,345	0	87,5
	pellet	1,177		
	supernatant	0		
2,06	whole lysate	1,411	0	96,9
	pellet	1,368		
	supernatant	0		
5,05	whole lysate	1,299	0	71,0
	pellet	0,922		
	supernatant	0		

Digitonin treatment – DLHex-DGJ detection				
18,12	whole lysate	1,628	0	62,5
	pellet	1,018		
	supernatant	0		
41,6	whole lysate	2,105	0	69,8
	pellet	1,058		
	supernatant	0,410		

'% soluble' was calculated as the enzymatic activity – or the chaperone concentration respectively – found in the supernatant in proportion to the enzymatic activity found in the pellet. Accordingly, '% recovery' was calculated as the sum of activity in pellet and supernatant in proportion to the whole cell lysate.

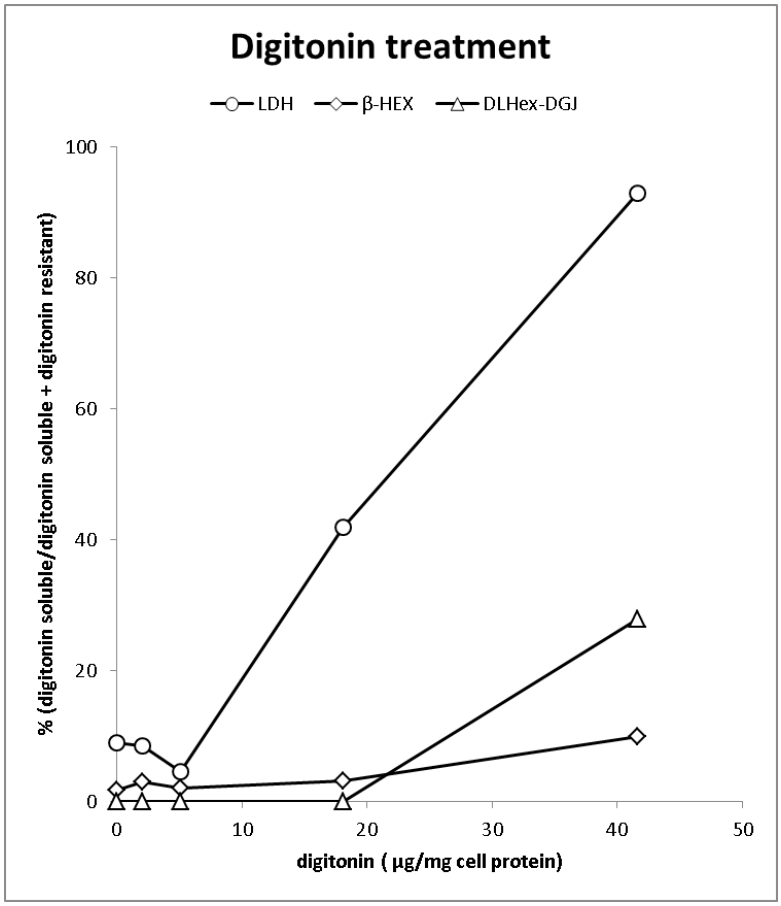

Figure 32: Cellular fractionation via digitonin treatment; Monitoring of cellular and organellar disruption via the activity of marker enzymes LDH and ß-HEX;

As can be seen in figure 32, at a concentration of 18,12 µg/mg digitonin the activity of lactate dehydrogenase in the supernatant increased significantly, while activity of ß-hexosaminidase and chaperone concentration stay unaffected. However, at a concentration of 41,6 µg/mg digitonin, both ß-hexosaminidase activity and chaperone concentration in the supernatant start to increase. This observation suggests an organellar, maybe even lysosomal, localization of DLHex-DGJ, while the concentrations in the cytoplasm is below the limit of detection.

5.3 Choice of model system for LSDs and chaperone tests

For apparent reasons, in most studies concerning human biological phenomena, from fundamental research to specific drug development – at least at some point of the scientific procedure – the use of model organisms has become an essential part of research.

Advantages and restrictions have to be evaluated thoroughly and highly depend on the specific research objectives. In the case of lysosomal storage disorders, human cell cultures have proven to be most versatile, but also a number of non-human models, be it mice or sheep, have been described [29].
While large animal models might be useful for the investigation of drug delivery and such, basal research often depends on the usage of systems with easier handling. While in some cases the focus lies on the best possible reproduction of the disease, other approaches demand the use of systems with higher throughput and more ease of use.

In the following section, the advantages and limitations of both fibroblast cultures and yeasts as potential novel model organism shall be discussed.

5.3.1 Fibroblast cultures

The method of culturing cells derived from patient tissue has been in use for several decades and holds several advantages over other techniques. Cell cultures are relatively easy to handle compared to animal models, and show more molecular resemblance to the host than basal model organisms such as yeast. Depending on the aim of distinct experiments, mammalian cell cultures therefore often present to be a reasonable compromise. Cell cultures in general have enormous significance for research on genetic diseases. for their use as models for the significance of enzymes and for the study of genetic biochemistry.
A main advantage in the case in the research of LSDs is the direct deduction of cultured cells from skin-stanzas of patients suffering from lysosomal storage disorders. This makes it possible to work on cells from patients with a distinct phenotype, a recorded case history with known characteristics and symptoms of the specific mutation.

This generally makes patient-derived cells beneficial as it avoids to manipulate the cells molecular-biologically in order for them to express the gene of interest comprising the mutation and hence potentially alter other cellular factors as well [29].
On the downside, however, skin fibroblasts often do not reflect the full characteristic of some diseases, as there are often tissue-specific effects as well. One point of criticism on the use of fibroblasts in LSD-research is the lack of typical levels of accumulated storage material compared to typically affected tissues [30]. Furthermore, work with fibroblasts is restricted by their relatively slow growth in comparison to simpler model systems as well as their elevated requirements in terms of growth medium and working conditions in general.

5.3.2 Yeast as a model organism

Yeasts are unicellular eukaryotic microorganisms within the kingdom of Fungi, but do not form a single group in terms of taxonomy of phylogeny. Several yeasts, *S*. *cerevisiae* and *Pichia pastoris* in particular, have been widely used in genetics and cell biology. As the molecular and genetic complexity of eucaroytes is astounding, it is just logical to analyze their internal workings without the added complications of multicellular development, but with the use of a unicellular species with utmost simplicity. Yeasts superbly serves as a model for many eukaryotes, including humans, in order to study fundamental cellular processes from cell division, cell cycle and DNA replication to recombination, cell signaling and metabolism [3].
Yeasts are robust and can be grown easily in non-complex culture media and under favorable conditions, the growth rate can reach levels almost similar to some bacteria.
For a long time it had been speculated that yeast could serve as an ideal model system for modern biology [31]. Its use increased steadily over the years, and not later than with the sequencing of the yeast genome being completed in 1996 [32], it eventually became a reference organism. Many features have made it a favorable organism especially for genetic studies: With an approximate count of 13,117,000 nucleotide pairs, the genome of *S.cerevisiae* comprises just a fraction of the genome of many other eucaryotes, and with a total number of 6300 encoded proteins, it is merely more complex than *Escherichia coli* for instance. A potent system of homologous recombination makes alterations in the

genome of *S.cerevisiae* especially easy and uncomplicated. This opened the way to novel insights to network interactions between regulatory proteins and the genes that code for them for instance.
Furthermore, yeasts have been exploited in different assays based on DNA microarrays, gene disruptions, protein localization and protein-protein interactions, e.g. via the yeast-two-hybrid system [33], [34].

However, the use of yeasts is not limited solely to the analysis of basal and fundamental cellular processes and regulatory interactions, as also the investigation on distinct human diseases is often accomplished with the utilization of a fungal model system. Interestingly, 40% of the yeast proteins show a similarity in sequence with at least one human protein and a striking 30% of genes that are known to be involved in human diseases have an ortholog in yeast [35]. The investigation on functional characteristics of defect human proteins in yeast may give hints to abnormal enzyme functions that might not have been detected solely from inspection of the protein sequence or other assays in humans [36]. Another approach for studying the function of human disease genes in yeast is the remediation of the underlying deficiency. As many missense mutations lead to decreased affinity for a substrate, compensation by increased dietary intake might lighten the defect [37]. As can be seen in chapter 5.3.3, this had been utilized in the study of CBS deficiency for instance.

Apart from all those applications, *S.cerevisiae* also is currently the best described model organism in the screening of drug sensitivity. As it – despite its simplicity – still provides a biologically intact system, chemical compounds can be analyzed in the context of a living cell. Due to its advantages in terms of life cycle and cultivating requirements it is especially well-suited for high-throughput methods. For drug screening approaches, yeasts provide a favorable model to investigate the effects of different compounds on cellular pathways as well as single proteins. The list of approaches ranges from gene overexpression studies, over haploinsufficiency screenings on to deletion of non-essential genes, all of which can be carried out easily and in a high-throughput manner in yeast. Yeast-based assays can further be used to express distinct human proteins and therefore screen for therapeutic compounds on a much broader scale than many other models [35], [38]. Especially the latter may be a promising approach in the screening of chemical

chaperones for the treatment of LSDs. The approach of heterologously expressing mutant forms of human lysosomal β-galactosidase in yeast is dealt with in chapter 5.3.5.

5.3.3 Yeast and human diseases

Up to this point, yeasts have been versatile models in the exercise of elucidating pathogenic mechanisms and defects in many different classes of human diseases, from neuropathogenic disorders to lysosomal diseases. Even insights in the process of human aging have become available via the utilization of fungal model organisms.

In case of peroxisomal biogenesis disorders (PBDs), which include for example Zellweger syndrome, infantile Refsum disease or neonatal adrenoleukodystrophy, screenings in yeast led to the identification of corresponding genes and the discovery of proteins essential for peroxisome biogenesis. As the disorders are widely associated with peroxisomal protein import, it was important to find the principles of the required machinery conserved in yeast. This might facilitate the identification of more proteins involved in peroxisomal biogenesis which have not yet been described, as defects may only cause a mild phenotype [39].

Prion diseases for instance may serve as an example were a mechanism is even better understood in yeast than in its mammalian counterparts. The phenomenon had been described first in the mid-18th century as a disease in sheep and goats. Later, counterparts in cattle, mice, chimpanzees and eventually humans were described. Finally, the concept of proteinaceous infectious particles was propagated by Stanley Prusiner in 1982 [40]. The latest definition describes those prions as a result of the conversion of proteins from their soluble to an aggregated and insoluble form, which is then capable of self-propagation as infectious agent [41].
In yeast, first prion-like proteins had been described as early as 1971. Up to now, several yeast proteins comprising a prion-forming domain have been found. As aggregate formation of those proteins leads to impairment of translational termination, this often results in the translation of nonsense-codons. As this in some cases might lead to beneficial recombinational expressions, it had been speculated that prion formation may play a role in evolutionary variation [42]. However, this concept could not have been fully

transferred to an explication of mammalian prion formation yet.

A whole set of neurodegenerative disorders, among which are Parkinson's disease, Alzheimer's disease and Chorea Huntington are studied with the aid of fungal model systems. In all of those cases, the accumulation of autophagic vesicles has been observed. In the case of Parkinson's disease (PD), it is the protein α-synuclein which plays a pivotal role between health and disease. In PD patients, one characteristic is the formation of so-called Lewy bodies in neurons, which are in large part composed of mutated α-synuclein protein. Even though not fully understood, the effects of those misfolded and aggregated proteins seem to lead to the distinct neurodegenerative appearance of the disease with subsequent reduced activity of dopamine-secreting cells [43]. Amongst other things, it could have been shown in *S.cerevisiae* that the expression of mutant α-synuclein severely affects the quality-control systems of the cell. It not only causes the accumulation of autophagic vesicles, but also impairs the ubiquitin-proteasome system, which normally removes misfolded proteins [44].

In a similar manner, the cause of Huntington's disease seems to lie in the expanded polyglutamine stretches at the amino terminus of the protein huntingtin. Aggregates of huntingtin seem to be a major cause of the disease but unlike in Parkinson's disease, the cause seemingly does not lie in the ubiquitin-proteasome system [43]. Heterologous expression of huntingtin in yeast showed increase in autophagic vesicle as well as increased activity of caspases and hence apoptotic behavior [45].
Furthermore, genome-wide screens in *S.cerevisiae* could have been used to identify genes that enhance the toxicity of mutant huntingtin as well as α-synuclein and could therefore give further insights into the cause of the disorder [46].

As for Alzheimer's disease, despite its widespread occurrence, the molecular mechanisms that cause the disorder are still insufficiently illuminated. As in Parkinson's and Huntington's disease, formation of proteinaceous aggregations seems to play a major role. In case of Alzheimer's disease, the misfolded protein – tau – seems to form fibrillar aggregates, termed β-amyloid plaques. Propagation of misfolded tau protein still remains a field of investigation, however, prion-like models have been suggested [47]. Elevated markers of the lysosomal integrity have been found in the brains of Alzheimer's disease

patients, once again proposing pivotal involvement of the regulation of the removal of neurotoxic material and the cells autophagic system [43]. Heterologous expression of tau protein in yeast leads to comparable features and physiognomies as in neuronal cells. This model could have been used to screen for AD preventatives with high throughput [48].

Classical Homocystinuria, also termed cystathionine beta synthase deficiency is an example of a human disorder were the application of a fungal screening systems revealed defects undisclosed by other methods [36]. The disorder is caused by recessive mutations in vitamin B6-dependent enzymes that lead to the development of a wide variety of symptoms with multisystemic involvement. As a better part of the mutations cause an increased Michaelis constant (K_m), meaning a lower binding affinity of the enzyme to its co-factor or substrate, a common treatment is the dietary compensation of the vitamin component of the co-enzyme [37]. As the cultivation of yeast under distinct substrate-deficient media conditions is relatively easy, the application of yeast-based models is manifest. Site-directed mutagenesis and the analysis of cognate yeast mutations of CBS B6-responsive alleles led to the finding of new therapeutic approaches, involving inducting of the heat-shock protein Hsp70 [49]. Further work of Singh et al. in *S.cerevisiae* also suggests chemical chaperone treatment to rescue mutant cystathionine beta-synthase [50].

Finally, as member of the group of neuronal ceroid lipofuscinosis (NCLs), batten disease illustrates a human disorder with the involvement of lysosomal enzymes were yeast can be used as a model system.
NCLs have been characterized by the accumulation of hydrophobic material mainly in the lysosomes of neurons. The genetic basis of batten disease lies in mutations of the *CLN3* gene, coding for the protein battenin, which is found in the membrane of lysosomes and endosomes, but whose functions is still unknown.
It could have been shown that the homolog of Cln3p in *S.cerevisiae* – Btn1p – shows 39% identity and 59% similarity to its human counterpart. Complementation experiments also revealed functional homology, allowing to use yeast to investigate gene products interacting with Btn1p [51].

5.3.4 The yeast vacuole

“Fungal vacuoles are acidic organelles with degradative and storage capabilities that have many similarities to mammalian lysosomes and plant vacuoles.” [52].
Just like mammalian lysosomes, the yeast vacuole is a centerpiece in the degradation of cellular content and has important functions in the regulation of the pH and the osmotic pressure as well as in the storage of amino acids and other components. Interestingly though, while in mammalian cells the lysosomal pH lies between 4,5 and 5, literature usually indicates a pH of 6 for yeast vacuoles [3].
It has become more and more evident that both mammalian lysosomes as well as fungal vacuoles are more than terminal compartments but rather play important roles in cellular regulation. Owing to their complaisance and submissiveness in terms of biochemical as well as genetic analysis, vacuoles of *S. cerevisiae* are used as models for trafficking processes in mammalian lysosomes [53].
Yeast vacuoles are particularly important in the study of the process of autophagy, where mainly damaged or redundant cellular content is recycled. This process, in all of its forms, from micro- to macroautophagy, pexophagy and piecemeal autophagy, plays an important role in cellular health and disease [3], [54].

But as good as a model for many cellular processes the yeast vacuole might be, there are some points where the difference to mammalian lysosomes becomes apparent:
As yeasts obviously do not have adipose tissue or a liver, the vacuoles of each cell not only have to handle degradation and turnover of molecules, but also have to take care of storage concerns. Concerning their appearance, yeast vacuoles, in contrast to mammalian lysosomes, can take up a significant amount of cell volume, that is, up to 20% depending on the conditions. [53].

5.3.5 Homologs of human β-galactosidase in yeast

One of the pivotal requirements when studying a specific enzyme in another organism is knowledge of the existence of potential homologs and orthologs. If existent, this may lead to new insights into the functionality of the original enzyme, but can on the other hand interfere in various ways when the enzyme is expressed herologously.

A feasible and quick way to do so – especially when the genome and proteome of the organisms of interest are as superbly mapped and analyzed as the ones from *Homo sapiens* and *Saccharomyces cerevisiae* – is the performance of various deductions of the BLAST alignment algorithm. As is commonly accepted, a sequence identity on genomic level of at least 30% or 10% on the amino-acid level of the encoded protein are limits for the assumption of homology.
As it turns out, this limit is neither reached when cDNA of the human *GLB1* gene is aligned against the *S.cerevisiae* genome nor when the amino-acid sequence of human lysosomal β-galactosidase is searched against the *Saccharomyces* protein database [55].
This confirms the common understanding that *S. cerevisiae* does not encode for a homolog of human lysosomal β-galactosidase, which makes it a usable organism for the expression and further examination of diverse forms of mutant *GLB1* genes.

In 1990, it had been shown by Toni Prezant that expression of the cDNA of the β chain of human lysosomal β-hexosaminidase in *S.cerevisiae* led to the formation of enzymatically active dimers which could have been demonstrated to be located in the yeast vacuole [56]. This finding is of utmost importance for the planning of heterologously expressing other human lysosomal proteins such as β-galactosidase, as it shows that the mannose-6-phosphate marker, required for the transport of lysosomal enzymes in humans but not necessary in *S.cerevisiae*, is not vital for proper vacuolar localization in yeast. However, the mechanisms on how lysosomal enzymes are recognized in yeast remain enigmatic.

Taken together, these presumptions tend to make the use of *S.cerevisae* as a model system to study lysosomal storage disorders in general and β-galactosidase-related disorders such as GM1 and MBD in specific a potential alternative at least in the field of fundamental research.

6 Discussion

In this master's thesis a novel method was developed to detect and quantify the pharmacological chaperone DLHex-DGJ, a derivative of 1-deoxygalactonojirimycin, via the use of high-resolution tandem mass spectrometry. Alongside with development and optimization of ionization and fragmentation conditions for the substance in its pure form, an extraction protocol was established which provides the possibility of measuring DLHex-DGJ in harvested human skin fibroblasts at adequate concentrations.

This method was further applied to determine the possible influence of chaperone concentration in culture medium to its intracellular recovery. A linear relationship between extra- and intracellular chaperone concentrations was found, without obvious saturation effect. Investigation on the dependency of incubation time to intracellular chaperone concentration suggests rapid uptake of DLHex-DGJ within the first hours. Preliminary results suggest lysosomal localization of intracellular chaperone.

6.1 Method development

The initial setting of the instruments had to be done completely from the beginning, since the substance had not been analyzed on this kind of mass spectrometer before.
Primarily, it was possible to detect the pharmacological chaperone DLHex-DGJ via direct injection. Through the high mass accuracy of the Q-Exactive system this was possible with a mass deviation of just around 1 to 1,5 ppm to the calculated mono-isotopic mass. With the initial detection accomplished, further optimization steps could have been approached.
Subsequently the conditions of the ESI probe and the Q-Exactive mass spectrometer were set in order to produce a maximum yield of the target ions for different flow rates. This process imposed no major problems, as every parameter of the ESI source and the mass spectrometer was optimized sequentially one by one. As for the sheath gas and auxiliary gas flow rate, those parameters were mainly modified in a concordant way, since too high differences between these two parameters were not considered favorable. As the achievement of a distinct fragmentation pattern had also been a main target, the

relatively higher sensitivity in positive ion mode was sacrificed for the favorable fragmentation pattern in negative ion mode.

Ergo secondly, it was possible to characterize the chaperone not only through the high mass accuracy of the Q-Exactive mass spectrometer, but also through the distinct fragmentation pattern in negative ion mode, where the dansyl fragment at 234,0590 m/z appears with high abundance.
The fragmentation pattern in positive ion mode was not considered beneficial for those needs, since it consisted of a relatively high number of fragment peaks with low abundance, of which not all could have been linked to the parent ion an a reasonable way.

As the target was to detect DLHex-DGJ in harvested skin fibroblasts, several extraction and clean-up steps had to be introduced in order to purify the substance and remove possibly disruptive cellular debris. The detection of DLHex-DGJ amongst the lipid fraction of harvested human skin fibroblasts could have been achieved through the application of high performance liquid chromatography. The Hpyersil^{TM} GOLD 50 x 2,1mm 3,0 µm C18 column was used based on the kind recommendation of Dr. Fauler, which was highly appreciated.
The gradient was first optimized for the appropriate elution of the chaperone, while further steps had been taken to quickly elute the remaining residues of the lipid extraction. This way, the run time could have been reduced to a total of 16 minutes.

The optimization of the lipid extraction turned out to be most troublesome, as even with the time-consuming introduction of a second and finally third extraction step, the overall recovery of DLHex-DGJ was as low as 60%. As measurements of the aqueous phase showed no significant retrieval of DLHex-DGJ, it is speculated that parts of the chaperone are held back in the protein layer.

Solid phase extraction on the other hand could be optimized to an extraction efficiency of well over 90% without the consumption of inconsiderable amounts of time or solvents.

The final calculation of the recovery rate resulted in approximately 55% of the chaperone to be found again after performing both extraction and clean-up steps. For this approach, the extraction efficiency was considered sufficient, as the typical working concentrations were well within the detectable range.

A possible way of handling the problem of chaperone loss in future experiments could be the establishment of an entirely different extraction procedure, possibly dealing better with the amphiphile character of the substance.

For quantification reasons, however, a general problem in this method is the absence of an internal standard. As the currently used method of external calibration might deal well enough with the problem of intra-day variations of the mass spectrometry equipment, alterations in the extraction steps as well as inter-day variations of the mass spectrometer generally cannot be sufficiently compensated for.
In this study, however, this was partly surmounted by the use of a higher number of replicative biological samples, which commonly improves the reproducibility.

6.2 Uptake of DLHex-DGJ in human skin fibroblasts

Previous studies on DLHex-DGJ proved it as a potent inhibitor of lysosomal β-galactosidase in vitro and as potentially effective pharmacological chaperone in vivo [21]. However, compared to other chaperones, such as NOEV [13], rather high doses (20-500 µM compared to 0,1-1 µM) have to be added to the culture medium for maximal effectiveness. Therefore, the uptake of DLHex-DGJ into the cells could be the limiting factor for its chaperone activity. If this was the case, the effective intracellular concentration should be markedly below the concentration in the culture medium.

The results of this work, however, cannot fully confirm this assumption. At a concentration of 13,067 ng/µl (20 µM) DLHex-DGJ in culture medium, an intracellular concentration of 8,99 ng/mg of cell protein was determined in p.R201C cells. Assuming a cellular protein content of 15% [3], the intracellular chaperone concentration can be estimated to be 10% of the concentration in the culture medium. Alternatively the intracellular concentration of DL-Hex-DGJ can also be estimated by multiplication of the number of cells per well ($3,8*10^5$ cells) with the average cell volume of fibroblast cells (10^3-10^4 µm³).Using the typical densities and volumes from literature, the intracellular concentration of DLHex-DGJ might be somewhere between 0,5 and 5 µM for a concentration of 20 µM in the culture media. Undoubtedly, further work is needed to confirm these rough estimations.

The second issue contradicting the theory of a limited chaperone uptake is the behavior at higher concentrations. In contrast to fluorinated DGJ derivatives, high concentrations of DLHex-DGJ do not result in a reduction of of ß-gal chaperoning but rather show a “saturation effect”. According to our results this is not caused by limitation of DLHex-DGJ uptake and may rather be related to nonspecific side effects. As fluorinated DGJ derivatives show a much more profound decline of chaperoning at high concentrations, these side effects appear to be comparatively mild. Time course of DLHex-DGJ uptake and release as well as resulting ß-gal activities has therefore also measured at high concentrations in the culture media.

6.3 Time-dependency of chaperone uptake

According to our results, the uptake of DLHex-DGJ into cells takes place in less than 6 hours. Even after two hours, more than 80% of the final intracellular concentration are reached. Upon removal of the chaperone from the culture medium, a reversed time-line can be observed in which 80% of the intracellular chaperone concentration are lost again after two hours.

The β-galactosidase activity within the first hours of exposure to DLHex-DGJ in contrast rises at a clearly lower rate. One can speculate that DLHex-DGJ only binds to and stabilizes newly synthesized enzymes without effect on pre-existing, misfolded enzymes. The rate of chaperone-induced rise of β-gal activity furthermore correlates well with the rate of enzyme synthesis observed by Van Diggelen et al. [57].

Taken a specific activity of 239,5 nmol/h/mg for the wildtype ([21]), untreated p.R201C cells show approx. 6,8% of wildtype activity, while after 24h of chaperone treatment, the activity rises to 12,2%. Extrapolation of this increase would lead to a theoretical activity of 28,4% after 96 hours of incubation. Indeed in the study of Fantur et al. ([21]) the actually measured value at this time-point was 29,3%. One can therefore assume that the increase in activity follows the described linear kinetics even after 24 hours. This again support the idea that only newly-synthesized enzymes are stabilized.

Further studies on the uptake kinetics with even shorter incubation times of under two hours would definitely be beneficial to further investigate the cellular uptake of DLHex-

DGJ. However, this was considered to be beyond the scope and time-frame of this master's thesis.

6.4 Subcellular localization of DLHex-DGJ

Digitonin “titration” experiments were used for preliminary experiments to give an estimate of the subcellular localization of DLHex-DGJ, using the marker enzymes lactate dehydrogenase and ß-hexosaminidase for the cytoplasm and lysosomes, respectively.

Both ß-hexosaminidase and DLHex-DGJ remained latent until to the highest digitonin-concentration, while at lower concentrations, LDH-activity was considerably elevated, while ß-hex-activity was at a basal level and DHLex-DGJ remained well below the limit of detection.

As the solubilization effect of digitonin primarily depends on the content of cholesterol in different membranes, the obtained data suggests a localization of DLHex-DGJ primarily in the lysosomal or endosomal compartments. Clearly this statement could be further strengthened with the measurement of a mitochondrial marker enzyme, which unfortunately was not available.

7 Outlook

With the availability of an optimized mass spectrometry assay for DL-Hex DGJ further experiments on the intracellular localization of DLHex-DGJ become feasible. These include an improved protocol for the cellular fractionation by density gradient ultracentrifugation to confirm the digitonin tritration results. This is of utter importance, as with the current method of just measuring ß-Hex, ß-Gal and LDH, no specific statement on the precise localization of DLHex-DGJ inside the cell can be made.

The centrifugation data have to be furthermore correlated with data on the time course of ß-gal precursor maturation under the influence of DL-Hex-DGJ and on data on their immunolocalisation. Commercial antibodies have recently become available, but their specificities have to be precisely defined, in order to correlate the data with the previously used non- commercial preparation ([21]) and to correlate the obtained preliminary results with previous findings.

Finally, the optimal concentrations for the chaperone-induced increase of enzyme activity seem to follow substantially different kinetics among various N-acyl analogues of DGJ (see [21], [23]). A further step will therefore be for instance to develop methods for the quantitation of the fluorinated compounds $Ph(TFM)_2$OHex-DGJ and $(TFM)_3$OHex-DGJ. Unlike DLHex-DGJ, where the chaperoning effect shows saturation at higher concentrations, the activation curves of these compounds are reduced at higher concentration [58].

Taken together, this current work will reveal insights into the cellular mechanisms of pharmacological chaperoning and their effects on target proteins. Together with recent data on the structure of the ß-gal protein (Ohto et al, 2013) this will enable us to design new more effective drugs, in particular to overcome the current limitations of mutation specificity.

8 References

[1] M. Sardiello, M. Palmieri, A. di Ronza, D. L. Medina, M. Valenza, V. A. Gennarino, C. Di Malta, F. Donaudy, V. Embrione, R. S. Polishchuk, S. Banfi, G. Parenti, E. Cattaneo, and A. Ballabio, "A gene network regulating lysosomal biogenesis and function.," *Science*, vol. 325, no. 5939, pp. 473–7, Jul. 2009.

[2] M. C. Micsenyi and S. U. Walkley, "General Aspects of Lysosomal Storage Diseases," in *Lysosomal Storage Disorders A Practival Guide*, A. Mehta and B. Winchester, Eds. Wiley-Blackwell, 2012, p. 197.

[3] B. Alberts, A. Johnson, J. Lewis, M. Raff, K. Roberts, and P. Walter, *Molecular Biology of the Cell, Fifth Edition*. 2008, p. 1601.

[4] Y. Yamamoto, C. A. Hake, B. M. Martin, K. A. Kretz, A. J. Ahern-Rindell, S. L. Naylor, M. Mudd, and J. S. O'Brien, "Isolation, characterization, and mapping of a human acid beta-galactosidase cDNA.," *DNA Cell Biol.*, vol. 9, no. 2, pp. 119–127, 1990.

[5] A. Pshezhetsky and M. Ashmarina, "Lysosomal multienzyme complex: biochemistry, genetics, and molecular pathophysiology.," *Prog. Nucleic Acid Res. Mol. Biol.*, vol. 69, pp. 81–114, 2001.

[6] U. Ohto, K. Usui, T. Ochi, K. Yuki, Y. Satow, and T. Shimizu, "Crystal structure of human β-galactosidase: structural basis of Gm1 gangliosidosis and morquio B diseases.," *J. Biol. Chem.*, vol. 287, no. 3, pp. 1801–12, Jan. 2012.

[7] "Genetics Home Reference." [Online]. Available: http://ghr.nlm.nih.gov/gene=GLB1. [Accessed: 30-Jun-2014].

[8] "NCBI - GLB1 galactosidase, beta 1 [homo sapiens (human)]." [Online]. Available: http://www.ncbi.nlm.nih.gov/gene/2720. [Accessed: 30-Jun-2014].

[9] "UniProtKB P16278 (BGAL_HUMAN)." [Online]. Available: www.uniport.org/uniprot/P16278#P16278-3. [Accessed: 08-Jul-2014].

[10] J. T. R. Clarke, "The Individual Diseases," in *Lysosomal Storage Disorders A Practival Guide*, A. Mehta and B. Winchester, Eds. 2012, p. 197.

[11] R. Giugliani, "The Individual Diseases," in *Lysosomal Storage Disorders A Practival Guide*, A. Mehta and B. Winchester, Eds. Wiley-Blackwell, 2012, p. 197.

[12] G. Parenti, "Treating lysosomal storage diseases with pharmacological chaperones: from concept to clinics.," *EMBO Mol. Med.*, vol. 1, no. 5, pp. 268–79, Aug. 2009.

[13] Y. Suzuki, "Chaperone therapy update: Fabry disease, GM1-gangliosidosis and Gaucher disease," *Brain Dev.*, vol. 35, no. 6, pp. 515–523, 2013.

[14] T. M. Cox, "Therapy and Patient Issues," in *Lysosomal Storage Disorders A Practival Guide*, A. Mehta and B. Winchester, Eds. 2012, p. 197.

[15] J. Fan, "A counterintuitive approach to treat enzyme deficiencies: use of enzyme inhibitors for restoring mutant enzyme activity," *Biol. Chem.*, vol. 389, no. 1, pp. 1–11, 2008.

[16] A. A. Watson, G. W. Fleet, N. Asano, R. J. Molyneux, and R. J. Nash, "Polyhydroxylated alkaloids - natural occurence adn therapeutic applications," *Phytochemistry*, vol. 56, no. 3,

pp. 265–295, 2001.

[17] F.-R. Heiker and A. M. Schueller, “Synthesis of d-galacto-1-deoxynojirimycin (1,5-dideoxy-1,5-imino-d-galactitol) starting from 1-deoxynojirimycin,” *Carb*, vol. 203, pp. 314–318, 1990.

[18] “Study of the Effects of Oral AT1001 (Migalastat Hydrochloride) in Patients With Fabry Disease.” [Online]. Available: http://clinicaltrials.gov/ct2/show/study/NCT00925301. [Accessed: 30-Jun-2014].

[19] Z. Yu, A. R. Sawkar, L. J. Whalen, C.-H. Wong, and J. W. Kelly, “Isofagomine- and 2,5-Anhydro-2,5-imino-d-glucitol-Based Glucocerebrosidase Pharmacological Chaperones for Gaucher Disease Intervention,” *J. Med. Chem.*, vol. 50, no. 1, pp. 94–100, Dec. 2006.

[20] A. Steiner, G. Schitter, A. Stütz, T. M. Wrodnigg, E. Paschke, and M. Tropak, “1-Deoxygalactonojirimycin-lysine hybrids as potent d-galactosidase inhibitors,” *Bioorg. Med. Chem.*, vol. 16, no. 24, pp. 10216–10220, 2008.

[21] K. Fantur, D. Hofer, G. Schitter, A. J. Steiner, B. M. Pabst, T. M. Wrodnigg, A. E. Stütz, and E. Paschke, “DLHex-DGJ, a novel derivative of 1-deoxygalactonojirimycin with pharmacological chaperone activity in human GM1-gangliosidosis fibroblasts,” *Mol. Genet. Metab.*, vol. 100, pp. 262–268, 2010.

[22] G. Schitter, E. Scheucher, A. J. Steiner, A. E. Stütz, M. Thonhofer, C. a Tarling, S. G. Withers, J. Wicki, K. Fantur, E. Paschke, D. J. Mahuran, B. a Rigat, M. Tropak, and T. M. Wrodnigg, “Synthesis of lipophilic 1-deoxygalactonojirimycin derivatives as D-galactosidase inhibitors.,” *Beilstein J. Org. Chem.*, vol. 6[1] G. Sc, p. 21, Jan. 2010.

[23] G. Schitter and A. Steiner, “Fluorous iminoalditols: a new family of glycosidase inhibitors and pharmacological chaperones,” *Chembiochem*, vol. 11, no. 14, pp. 2026–2033, 2010.

[24] S. Moldoveanu and V. David, *Essentials in modern HPLC separations*. Elsevier, 2012, p. 550.

[25] J. H. Gross, *Massenspektrometrie - Ein Lehrbuch*. Springer Spektrum, 2013, p. 820.

[26] “Q Exactive Scientific Resources.” [Online]. Available: www.planetorbitrap.com/q-exactive#tab:resources. [Accessed: 01-Jul-2014].

[27] A. M. Janski and N. W. Cornell, “Subcellular distribution of enzymes determined by rapid digitonin fractionation of isolated hepatocytes.,” *Biochem. J.*, vol. 186, no. 2, pp. 423–9, Feb. 1980.

[28] Z. Wu, W. Gao, M. A. Phelps, D. Wu, D. D. Miller, and J. T. Dalton, “Favorable effects of weak acids on negative-ion electrospray ionization mass spectrometry,” *Anal. Chem.*, vol. 76, no. 3, pp. 839–847, 2004.

[29] H. Zigdon, A. Meshcheriakova, and A. H. Futerman, “From sheep to mice to cells: Tools for the study of the sphingolipidoses.,” *Biochim. Biophys. Acta*, vol. 1841, no. 8, pp. 1189–1199, Mar. 2014.

[30] T. Farfel-Becker, E. Vitner, H. Dekel, N. Leshem, I. B. Enquist, S. Karlsson, and A. H. Futerman, “No evidence for activation of the unfolded protein response in neuronopathic models of Gaucher disease.,” *Hum. Mol. Genet.*, vol. 18, no. 8, pp. 1482–8, Apr. 2009.

[31] D. Botstein and G. R. Fink, “Yeast : An Experimental Organism Modern Biology,” *Science (80-.).*, vol. 240, no. 4858, pp. 1439–1443, 1988.

[32] A. Goffeau, B. G. Barrell, H. Bussey, R. W. Davis, B. Dujon, H. Feldmann, F. Galibert, J. D.

Hoheisel, C. Jacq, M. Johnston, E. J. Louis, H. W. Mewes, Y. Murakami, P. Philippsen, H. Tettelin, and S. G. Oliver, “Life with 6000 Genes,” *Science (80-.).*, vol. 274, no. 25, pp. 546–567, 1996.

[33] P. O. Brown and D. Botstein, “Exploring the new world of the genome with DNA microarrays.,” *Nat. Genet.*, vol. 21, no. 1 Suppl, pp. 33–7, Jan. 1999.

[34] P. Uetz, L. Giot, G. Cagney, T. a Mansfield, R. S. Judson, J. R. Knight, D. Lockshon, V. Narayan, M. Srinivasan, P. Pochart, a Qureshi-Emili, Y. Li, B. Godwin, D. Conover, T. Kalbfleisch, G. Vijayadamodar, M. Yang, M. Johnston, S. Fields, and J. M. Rothberg, “A comprehensive analysis of protein-protein interactions in Saccharomyces cerevisiae.,” *Nature*, vol. 403, no. 6770, pp. 623–7, Feb. 2000.

[35] C. M. Sturgeon, D. Kemmer, H. J. Anderson, and M. Roberge, “Yeast as a tool to uncover the cellular targets of drugs.,” *Biotechnol. J.*, vol. 1, no. 3, pp. 289–98, Mar. 2006.

[36] D. Botstein and G. R. Fink, “Yeast: an experimental organism for 21st Century biology.,” *Genetics*, vol. 189, no. 3, pp. 695–704, Nov. 2011.

[37] B. N. Ames, I. Elson-Schwab, and E. A. Silver, “High-dose vitamin therapy stimulates variant enzymes with decreased coenzyme binding affinity (increased K(m)): relevance to genetic disease and polymorphisms.,” *Am. J. Clin. Nutr.*, vol. 75, no. 4, pp. 616–58, Apr. 2002.

[38] A. X. S. Santos and H. Riezman, “Yeast as a model system for studying lipid homeostasis and function.,” *FEBS Lett.*, vol. 586, no. 18, pp. 2858–67, Aug. 2012.

[39] S. Nagotu, V. C. Kalel, R. Erdmann, and H. W. Platta, “Molecular basis of peroxisomal biogenesis disorders caused by defects in peroxisomal matrix protein import,” *Biochim. Biophys. Acta*, vol. 1822, no. 9, pp. 1326–1336, 2012.

[40] S. Prusiner, “Novel Proteinaceous Infectious Particles cause Scrapie,” *Science (80-.).*, vol. 216, no. 4542, pp. 136–144, 1982.

[41] S. M. Cascarina and E. D. Ross, “Yeast prions and human prion-like proteins: sequence features and prediction methods.,” *Cell. Mol. Life Sci.*, vol. 71, no. 11, pp. 2047–63, Jun. 2014.

[42] A. Aguzzi and M. Polymenidou, “Mammalian prion biology: one century of evolving concepts.,” *Cell*, vol. 116, no. 2, pp. 313–27, Jan. 2004.

[43] T. Shintani and D. J. Klionsky, “Autophagy in Heatlth and Disease: A Double-Edged Sword,” *Science (80-.).*, vol. 306, no. 5698, pp. 990–995, 2004.

[44] T. F. Outeiro and S. Lindquist, “Yeast cells provide insight into alpha-synuclein biology and pathobiology.,” *Science*, vol. 302, no. 5651, pp. 1772–5, Dec. 2003.

[45] S. Krobitsch and S. Lindquist, “Aggregation of huntingtin in yeast varies with of the Length of the Polyglutamine Expansion and the Expression of Chaperone Proteins,” *Proc. Natl. Acad. Sci. U. S. A.*, vol. 97, no. 4, pp. 1589–1594, 2000.

[46] S. Wiuingham, T. F. Outeiro, M. J. Devit, S. L. Lindquist, and P. J. Muchowski, “Yeast Genes That Enhance the Toxîcity of a Mutant Huntingtin Fragment or a-Synuclein,” *Science (80-.).*, vol. 302, no. 5, pp. 1769–1773, 2003.

[47] M. Cushman, B. S. Johnson, O. D. King, A. D. Gitler, and J. Shorter, “Prion-like disorders: blurring the divide between transmissibility and infectivity.,” *J. Cell Sci.*, vol. 123, no. Pt 8, pp. 1191–201, Apr. 2010.

[48] A. Porzoor and I. G. Macreadie, “Application of yeast to study the tau and amyloid-β abnormalities of Alzheimer’s disease.,” *J. Alzheimers. Dis.*, vol. 35, no. 2, pp. 217–25, Jan. 2013.

[49] L. R. Singh, S. Gupta, N. H. Honig, J. P. Kraus, and W. D. Kruger, “Activation of Mutant Enzyme Function In Vivo by Proteasome Inhibitors and Treatments that Induce Hsp70,” *PloS Genet.*, vol. 6, no. 1, pp. 1–10, 2010.

[50] L. R. Singh, X. Chen, V. Koz, and W. D. Kruger, “Chemical chaperone rescue of mutant human cystathionine b -synthase,” *Mol. Genet. Metab.*, vol. 91, pp. 335–342, 2007.

[51] D. A. Pearce and F. Sherman, “A yeast model for the study of Batten disease,” *Proc. Natl. Acad. Sci. U. S. A.*, vol. 95, no. 12, pp. 6915–6918, 1998.

[52] S. C. Li and P. M. Kane, “The Yeast Lysosome-Like Vacuole: Endpoint and Crossroads,” *Biochim. Biophys. Acta*, vol. 1793, no. 4, pp. 650–663, 2009.

[53] J. Armstrong, “Yeast vacuoles: more than a model lysosome.,” *Trends Cell Biol.*, vol. 20, no. 10, pp. 580–5, Oct. 2010.

[54] C. P. Kurtzman, J. W. Fell, and T. Boekhout, *The Yeasts, a Taxonomic Study Volume 1*. 2011, p. 2384.

[55] “Saccharomyces Genome Database.” [Online]. Available: www.yeastgenome.org. [Accessed: 18-Jul-2014].

[56] T. R. Prezant, “Expression of Human Lysosomal B-Hexosaminidase in Yeast Vacuoles,” *Biochem. Biophys. Res. Commun.*, vol. 170, no. 1, pp. 383–390, 1990.

[57] O. Van Diggelen, A. Schram, M. Sinnott, P. Smith, D. Robinson, and H. Galjaard, “Turnover of beta-galactosidase in fibroblasts from patients with genetically different types of beta-galactosidase deficiency,” *Biochem. J.*, vol. 200, no. 1, pp. 143–151, 1981.

[58] K. Fantur, T. M. Wrodnigg, A. E. Stütz, B. M. Pabst, and E. Paschke, “Fluorous iminoalditols act as effective pharmacological chaperones against gene products from GLB1 alleles causing GM1-gangliosidosis and Morquio B disease,” *J. Inherit. Metab. Dis.*, vol. 35, pp. 495–503, 2012.

[59] “Glycosphingolipids - LipidomicsWiki - LipidomicNet.” [Online]. Available: http://www.lipidomicnet.org/index.php/Glycosphingolipids. [Accessed: 30-Jun-2014].

[60] PerkinElmer, “ChemDraw Ultra.” CambridgeSoft, 2013.

[61] “Schematic of the Q-Exactive.” [Online]. Available: www.planetorbitrap.com/q-exactive#tab:schematic. [Accessed: 01-Jul-2014].